

CHAPTER III

THERMOCLINE CHARACTERISTICS OFF THE WEST COAST OF INDIA

3.1 INTRODUCTION

Seasonal variability in the temperature field is quite large off the west coast of India where vertical motions are significant (Sharma,1968,1978; Banse,1968; Darbyshare,1967; Narayana Pillai et al.,1980; Shetye,1984). The annual cycle of temperature and density fields off the west coast of India suggest the occurrence of upwelling during March-August and sinking during November to February (Sharma,1966;1968;1978; Narayana Pillai et al.,1980; Mathew,1981; Shetye,1984; Hareesh Kumar,1994). The upwelling/sinking commences in the southern region and progresses northward with time lags of the order of few months (Hareesh Kumar,1994). During the periods of upwelling a northward flowing undercurrent develops at the shelf edge which brings waters from the equatorial Indian Ocean (Antony,1990). The major transformations due to upwelling are the upward displacement of thermocline with an increase/decrease in the gradient of the upper/lower thermocline while sinking causes downward displacement of thermocline.

One of the notable features of the watermass structure in the eastern Arabian Sea is the presence of a high saline watermass, the Arabian Sea High Salinity Watermass, throughout the year (Hareesh Kumar,1994). Another prominent watermass found in this region is the low saline waters from the Bay of Bengal and Equatorial Indian Ocean during winter

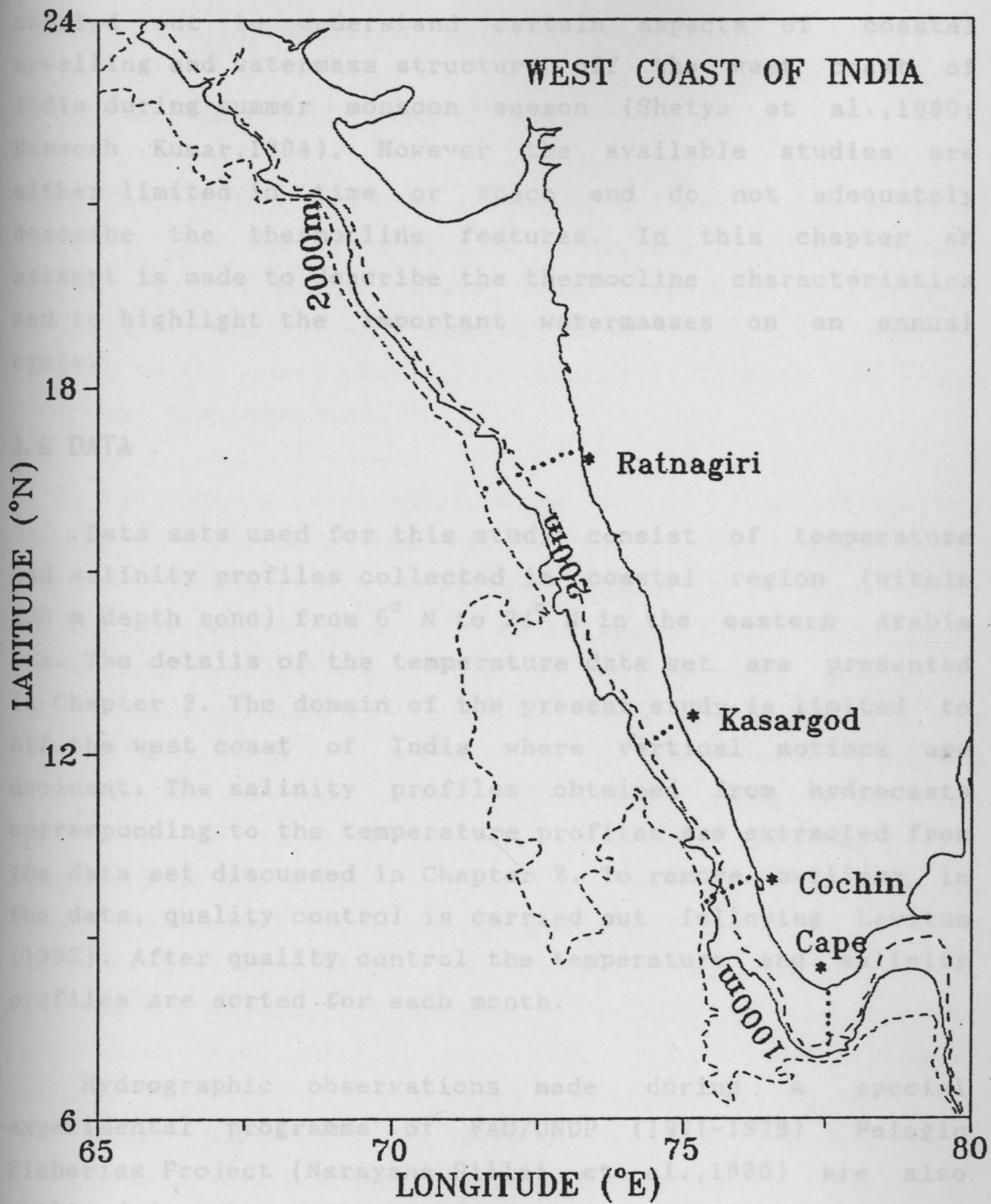


Fig. 3.1 Station location map

(Darbyshire,1967; Wyrтки,1971; Johannessen et al.,1981; Pankajakshan and Ramaraju,1987). Several studies have been carried out to understand certain aspects of coastal upwelling and watermass structure off the west coast of India during summer monsoon season (Shetye et al.,1990; Hareesh Kumar,1994). However the available studies are either limited in time or space and do not adequately describe the thermocline features. In this chapter an attempt is made to describe the thermocline characteristics and to highlight the important watermasses on an annual cycle.

3.2 DATA

Data sets used for this study consist of temperature and salinity profiles collected in coastal region (within 200 m depth zone) from 6° N to 24° N in the eastern Arabia Sea. The details of the temperature data set are presented in Chapter 2. The domain of the present study is limited to off the west coast of India where vertical motions are dominant. The salinity profiles obtained from hydrocasts corresponding to the temperature profiles are extracted from the data set discussed in Chapter 2. To remove outliers in the data, quality control is carried out following Levitus (1982). After quality control the temperature and salinity profiles are sorted for each month.

Hydrographic observations made during a special experimental programme of FAO/UNDP (1971-1978) Pelagic Fisheries Project (Narayana Pillai et al.,1980) are also utilised for the present work to study the cross-shore variations. During this programme hydrographic measurements were carried out at selected stations normal to the west coast of India (Fig.3.1). The same stations were occupied at

least seven to eight times in a year. This provided a very good data base to study the seasonal evolution of the thermocline characteristics off the west coast of India.

3.3 CROSS-SHELF VARIATIONS OF TEMPERATURE FIELD

It is well known that large variations in the thermal structure are mainly related to nearshore-offshore dynamic processes. In order to study these aspects, the monthly cross shelf variation of temperature at selected locations normal to the coast (Ratnagiri, Kasargod, Cochin, and Cape Comorin) are presented.

The monthly cross-shelf variation of temperature off Ratnagiri shows deep thermocline (>60m) from January to March. The temperature above the thermocline is about 27°C during this period (Fig.3.2). In this zone, isotherms slope upwards towards the coast from May to December indicating upwelling. During this period, temperature gradient is strong ($\cong 0.36^{\circ}\text{Cm}^{-1}$ in October) in the upper thermocline ($\cong 50\text{m}$) close to the coast. The upward movement of the isotherms is inhibited by the downward mechanical and buoyant mixing processes (Hastenrath and Lamb, 1979; Mohan Kumar, 1991) resulting in strong gradient. A mild downward slope of isotherms below 125m is seen in December. This is an indirect evidence of the northward flowing undercurrent associated with coastal upwelling which significantly reduces the vertical temperature gradient ($<0.04^{\circ}\text{C m}^{-1}$) in the lower part of the thermocline. The intensity of upwelling is maximum during August to September resulting in the formation of cold upper layer temperatures ($<27^{\circ}\text{C}$ near the coast). The isotherms descend in January indicating the sinking process in the thermocline. During this period a four fold reduction in the temperature gradient ($0.36^{\circ}\text{Cm}^{-1}$

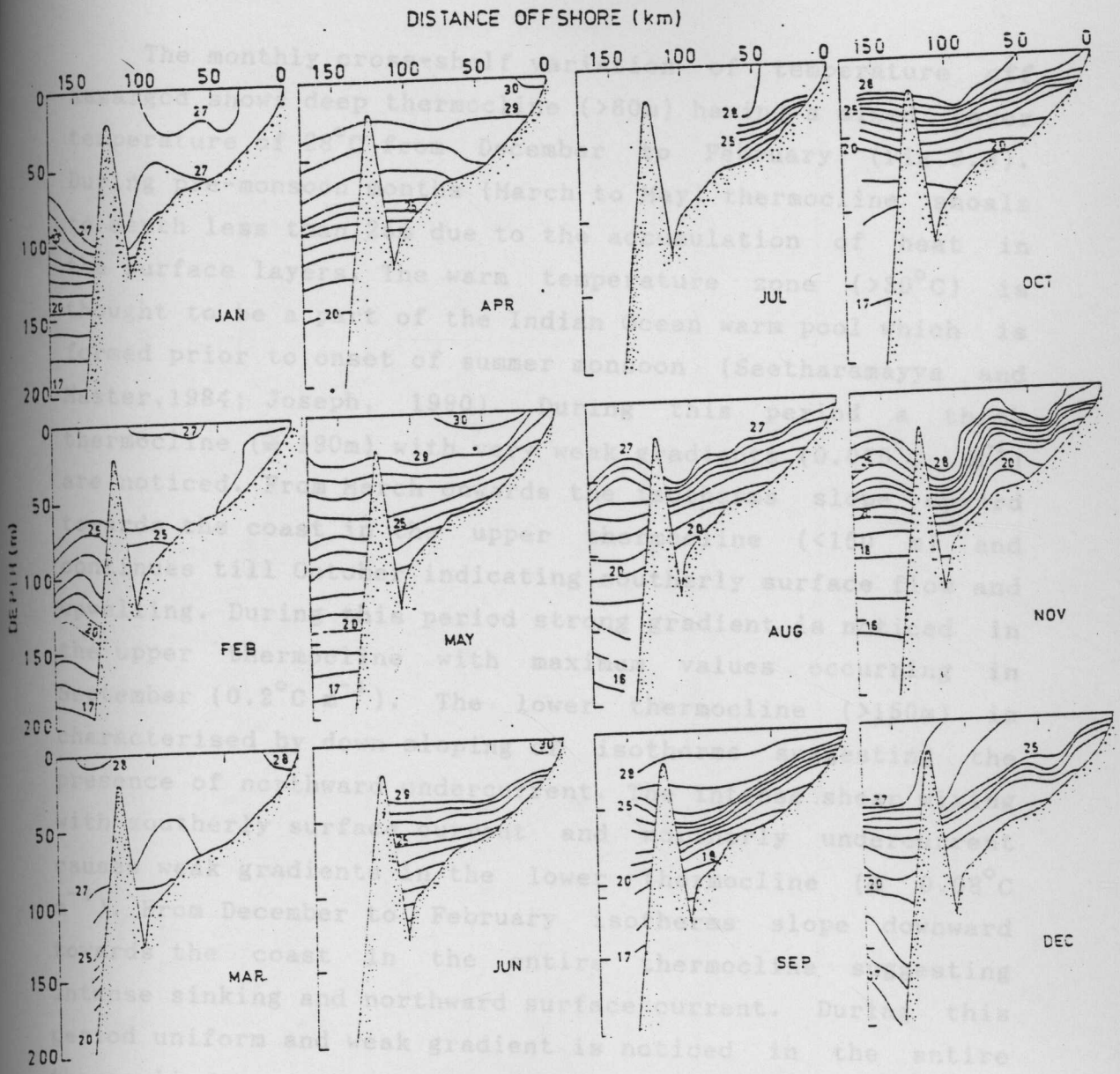


Fig. 3.2 Monthly Cross-shelf variations of temperature off Ratnagiri (°C)

to $0.08^{\circ}\text{C m}^{-1}$) within the thermocline is observed. This suggests that with the evolution of sinking process the thermocline diffused considerably. The diffused thermocline can be traced till upwelling gathers momentum.

DISTANCE OFFSHORE (km)

The monthly cross-shelf variation of temperature off Kasargod shows deep thermocline ($>60\text{m}$) having a mixed layer temperature of 28°C from December to February (Fig.3.3). During pre-monsoon months (March to May) thermocline shoals to depth less than 25m due to the accumulation of heat in the surface layers. The warm temperature zone ($>30^{\circ}\text{C}$) is thought to be a part of the Indian Ocean warm pool which is formed prior to onset of summer monsoon (Seetharamayya and Master, 1984; Joseph, 1990). During this period a thick thermocline ($\cong 190\text{m}$) with very weak gradients ($0.075^{\circ}\text{C m}^{-1}$) are noticed. From March onwards the isotherms slope upward towards the coast in the upper thermocline ($<150\text{ m}$) and continues till October indicating southerly surface flow and upwelling. During this period strong gradient is noticed in the upper thermocline with maximum values occurring in September ($0.2^{\circ}\text{C m}^{-1}$). The lower thermocline ($>150\text{m}$) is characterised by down sloping of isotherms suggesting the presence of northward undercurrent. The intense shear mixing with southerly surface current and northerly undercurrent causes weak gradients in the lower thermocline ($\cong 0.08^{\circ}\text{C m}^{-1}$). From December to February isotherms slope downward towards the coast in the entire thermocline suggesting intense sinking and northward surface current. During this period uniform and weak gradient is noticed in the entire thermocline.

A deep thermocline ($>100\text{m}$) with surface layer temperatures of 28°C is observed in December off Cochin Fig.(3.4). The influence of intense surface heating during

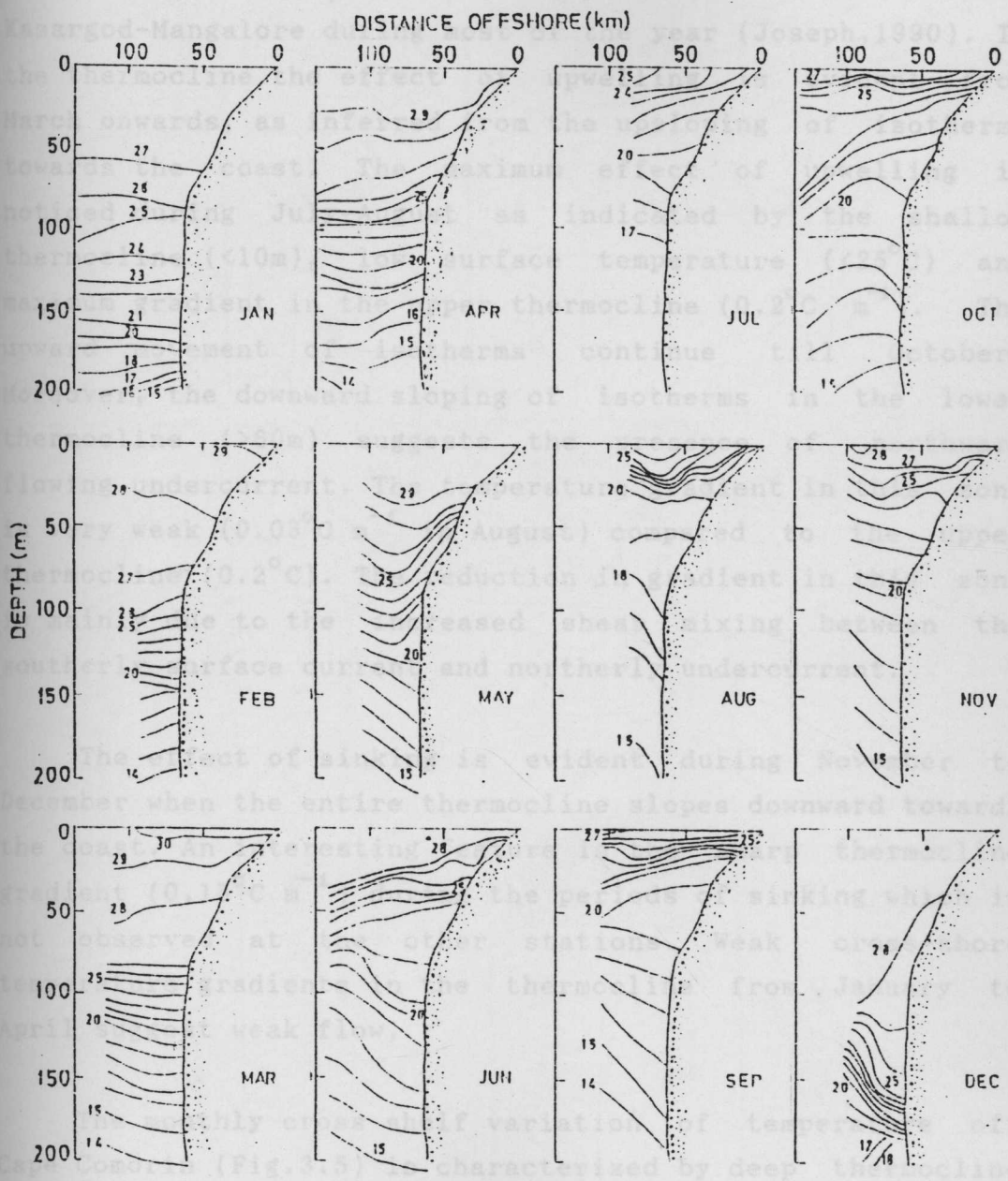


Fig. 3.3 Monthly cross-shelf variations of temperature off Kasargod($^{\circ}\text{C}$)

pre-monsoon period is reflected in the surface layer with temperature exceeding 29°C between March and May. The surface layer temperature off Cochin is lower (by $\cong 1^{\circ}\text{C}$) than that of Kasargod during this period probably because the Indian Ocean warm water pool is centered off Kasargod-Mangalore during most of the year (Joseph, 1990). In the thermocline the effect of upwelling is evident from March onwards, as inferred from the upsloping of isotherms towards the coast. The maximum effect of upwelling is noticed during July-August as indicated by the shallow thermocline ($<10\text{m}$), low surface temperature ($<25^{\circ}\text{C}$) and maximum gradient in the upper thermocline ($0.2^{\circ}\text{C m}^{-1}$). The upward movement of isotherms continue till October. Moreover, the downward sloping of isotherms in the lower thermocline ($>60\text{m}$) suggests the presence of northward flowing undercurrent. The temperature gradient in this zone is very weak ($0.03^{\circ}\text{C m}^{-1}$ in August) compared to the upper thermocline (0.2°C). The reduction in gradient in this zone is mainly due to the increased shear mixing between the southerly surface current and northerly undercurrent.

The effect of sinking is evident during November to December when the entire thermocline slopes downward towards the coast. An interesting feature is the sharp thermocline gradient ($0.15^{\circ}\text{C m}^{-1}$) during the periods of sinking which is not observed at the other stations. Weak cross-shore temperature gradients in the thermocline from January to April suggest weak flow.

The monthly cross shelf variation of temperature off Cape Comorin (Fig. 3.5) is characterised by deep thermocline ($>70\text{m}$) with near surface temperature more than 27°C during December to January. It may be noted that depression of isotherms with sharp thermal gradient ($0.3^{\circ}\text{C m}^{-1}$) is

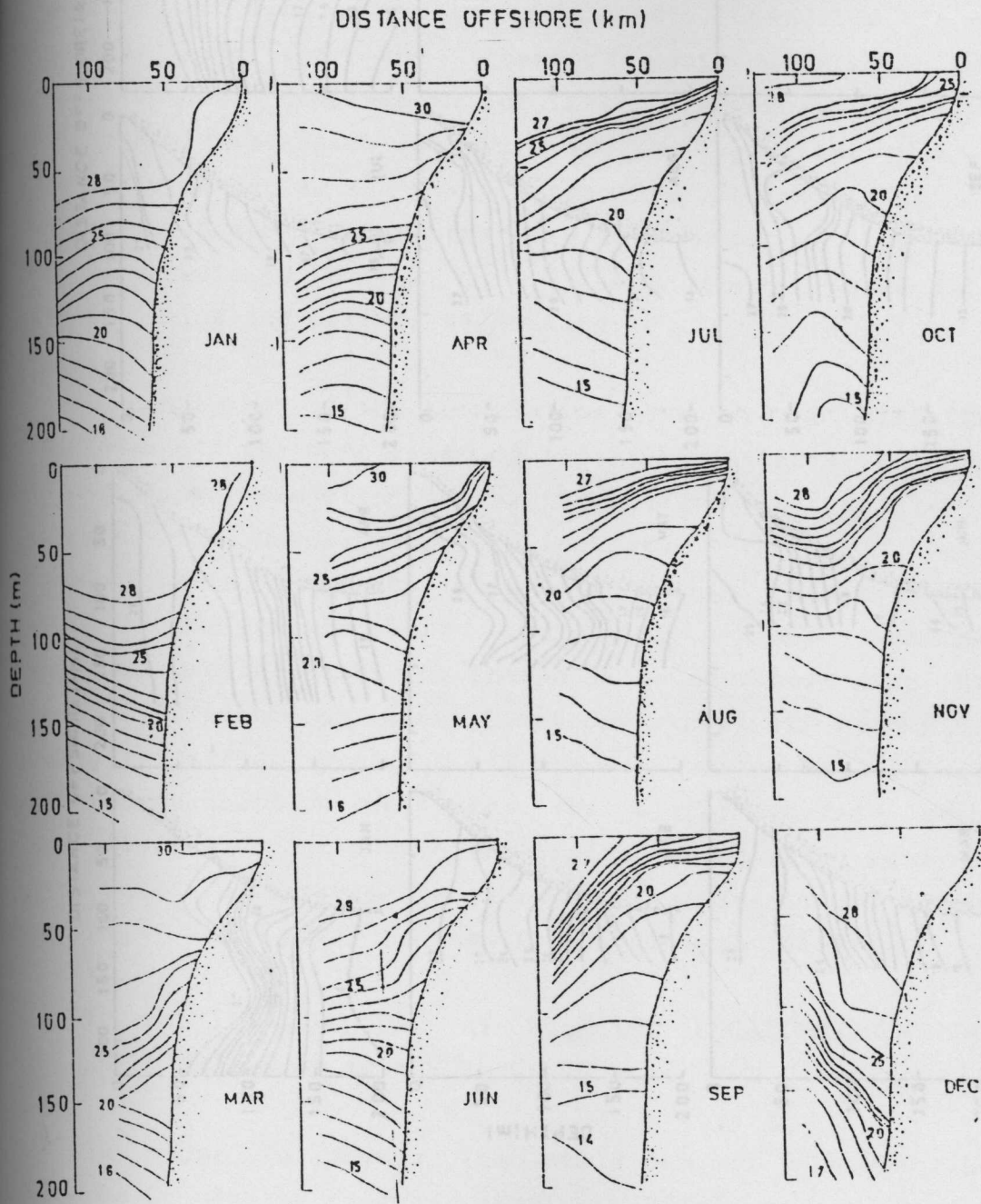


Fig. 3.4 Monthly cross-shelf variations of temperature off Cochin ($^{\circ}\text{C}$)

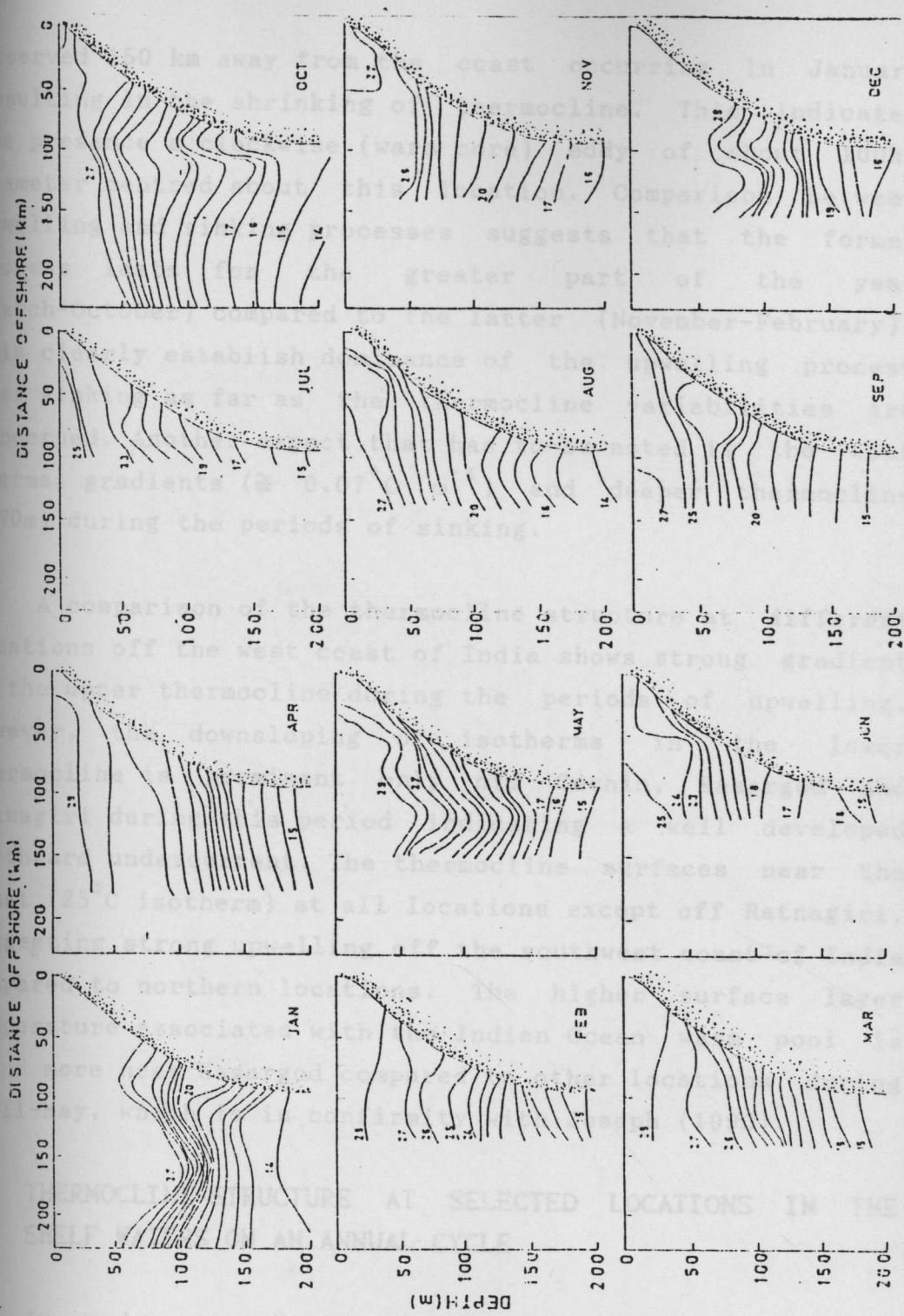


Fig. 3.5 Monthly cross-shelf variations of temperature off Cape Comorin ($^{\circ}\text{C}$)

In order to obtain the evolution of thermocline features in coastal regions (depths $< 200\text{m}$) on an annual scale, depth-time sections of monthly mean temperatures at selected locations off the west coast of India (Fig.3.1) are

observed 150 km away from the coast occurring in January resulting in the shrinking of thermocline. This indicates the presence a clockwise (warm core) eddy of about 100km diameter centred about this location. Comparison between upwelling and sinking processes suggests that the former process lasts for the greater part of the year (March-October) compared to the latter (November-February). This clearly establish dominance of the upwelling process over sinking as far as the thermocline variabilities are concerned. Another aspect that has to be noted is the weak thermal gradients ($\cong 0.07^{\circ}\text{C m}^{-1}$) and deeper thermocline (>70m) during the periods of sinking.

A comparison of the thermocline structure at different locations off the west coast of India shows strong gradient in the upper thermocline during the periods of upwelling. However, the downsloping of isotherms in the lower thermocline is prominent only off Cochin, Kasargod and Ratnagiri during this period indicating a well developed northward undercurrent. The thermocline surfaces near the coast (25°C isotherm) at all locations except off Ratnagiri, suggesting strong upwelling off the southwest coast of India compared to northern locations. The higher surface layer temperature associated with the Indian Ocean warm pool is found more near Kasargod compared to other locations during April-May, which is in confirmity with Joseph (1990).

3.4 THERMOCLINE STRUCTURE AT SELECTED LOCATIONS IN THE SHELF WATERS ON AN ANNUAL CYCLE

In order to obtain the evolution of thermocline features in coastal regions (depths <200m) on an annual cycle, depth-time sections of monthly mean temperatures at selected locations off the west coast of India (Fig.3.1) are

presented in Fig.3.6.

The isotherms start ascending in the thermocline zone at all locations from pre-monsoon period suggesting the commencement of upwelling. However, this process is found to occur with certain time lag. It can be seen that isotherms in the thermocline zone off Cape Comorin

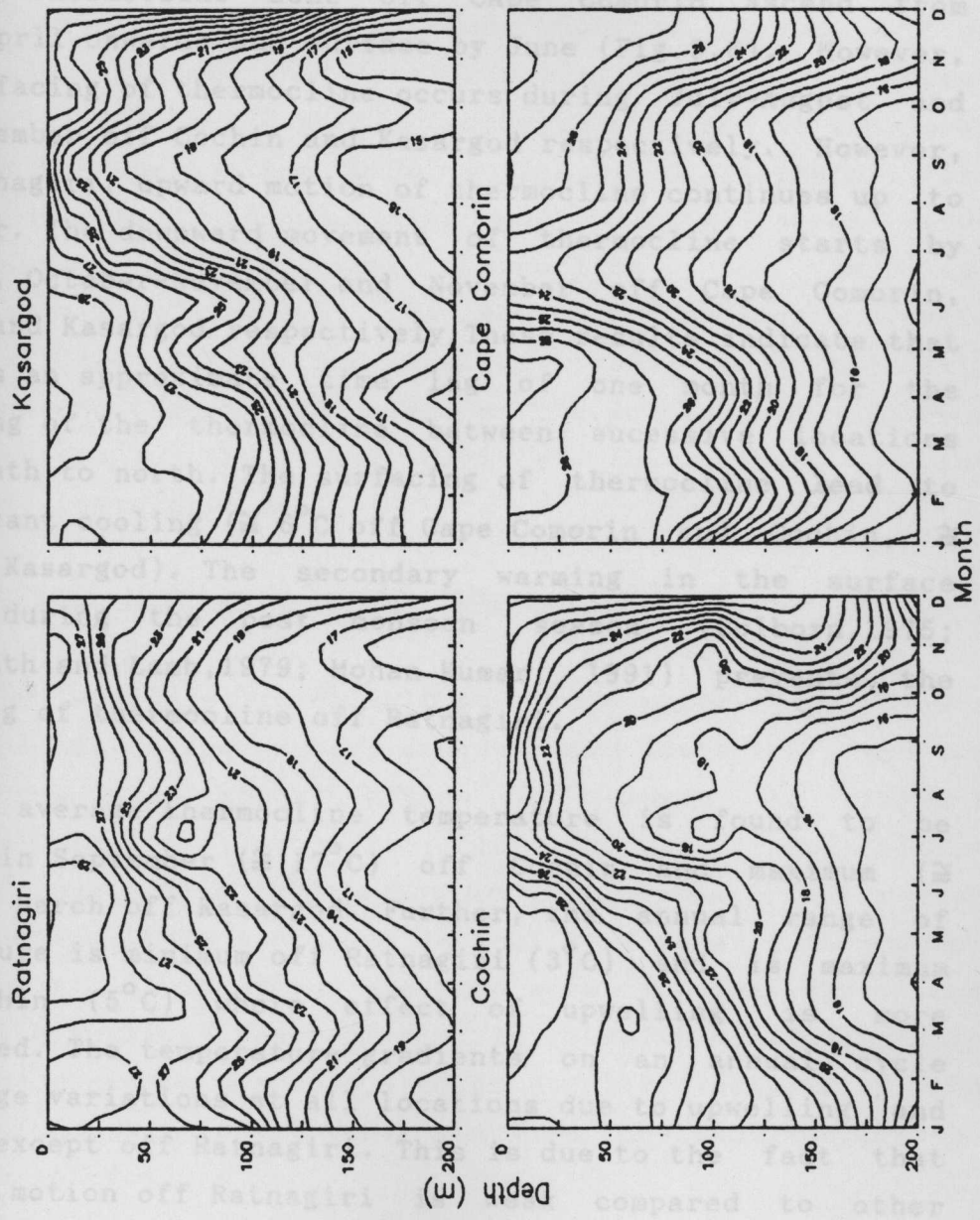


Fig. 3.6 Depth-time sections of temperature at selected locations (°C)

presented in Fig.3.6.

The isotherms start ascending in the thermocline zone at all locations from pre-monsoon period suggesting the commencement of upwelling. However, this process is found to occur with certain time lag. It can be seen that isotherms in the thermocline zone off Cape Comorin ascend from March/April onwards and surface by June (Fig.3.6). However, the surfacing of thermocline occurs during July-August and in September off Cochin and Kasargod respectively. However, off Ratnagiri, upward motion of thermocline continues up to November. The downward movement of thermocline starts by October, October-November and November off Cape Comorin, Cochin and Kasargod respectively. These results indicate that there is an approximate time lag of one month for the surfacing of the thermocline between successive locations from south to north. The surfacing of thermocline lead to significant cooling ($\cong 6^{\circ}\text{C}$ off Cape Comorin and Cochin, $\cong 4^{\circ}\text{C}$ off Kasargod). The secondary warming in the surface layers during the post monsoon season (Colborn,1975; Hastenrath and Lamb,1979; Mohan Kumar, 1991) prevents the surfacing of thermocline off Ratnagiri.

The average thermocline temperature is found to be minimum in September ($\cong 17^{\circ}\text{C}$) off Cochin and maximum ($\cong 24^{\circ}\text{C}$) in March off Kasargod. Further, the annual range of temperature is minimum off Ratnagiri (3°C) and is maximum off Cochin (5°C) where effect of upwelling is more pronounced. The temperature gradients on an annual cycle show large variations at all locations due to upwelling and sinking except off Ratnagiri. This is due to the fact that vertical motion off Ratnagiri is weak compared to other stations (where the thermocline does not surfaces). At all locations the gradients are strong in the upper thermocline

during the upwelling periods. Reduction in the gradient in the lower thermocline is due to the presence of northward flowing undercurrent. This can be inferred from the depth-time section of temperature (Fig.3.6) also where spreading of isotherms are noticed in the depth range of 80-150m.

Another interesting feature noticed is the large vertical displacement of isotherms (Fig.3.6) in the upper thermocline ($\cong 110\text{m}$ for 23°C isotherm) compared to the lower part of the thermocline ($\cong 30\text{ m}$ for 16°C isotherm). The combined effect of upwelling and sinking causes large displacement in the upper thermocline. The increased vertical mixing caused by the southerly surface currents (KNMI, 1952; Cutler and Swallow, 1984) and northerly undercurrent (Antony,1990) reduces the vertical displacement of isotherms in the lower part of thermocline, thereby reducing its amplitudes.

3.5 VERTICAL MOVEMENTS IN THE THERMOCLINE

The analysis reveals that the upper and lower thermoclines undergo upward and downward motions of varying magnitudes in an annual cycle. To compute the rate of vertical motion (Table 3.1) in the upper and lower thermoclines 23° and 18°C isotherms were chosen. The reason for choosing these isotherms is that they persist throughout the year at all locations and are seen in the upper and lower thermoclines respectively. It is worth mentioning here that there are no previous studies available describing the vertical motions in the upper and lower thermoclines for the west coast of India.

The rate (per month) of upward movement of 23°C

isotherm is 30m (110m in April to 20m in July) off Cape Comorin. The corresponding values are 23m (130m in February to 15m in July), 20m (125m in March to 10m in September) and 11m (130m in March to 40m in November) off Cochin, Kasargod and Ratnagiri respectively. Contrary to upward movement, the downward movement of this isotherm is found to be rapid (Table 3.1). For instance, the rate of downward movement is 33m (65m in September to 130m in November) and 78m (15m in September to 170m in November) off Cape Comorin and Cochin respectively. The corresponding values are 30m (13m in September to 103 in December) off Kasargod and 23m (40m in October to 110m in January) off Ratnagiri.

TABLE 3.1
Rates of Vertical movement 23°C and 18°C isotherms

Locations	Rate (m month ⁻¹)	
	23°C	18°C
Cape	30 (33)	17 (31)
Cochin	23 (78)	21 (72)
Kasargod	20 (30)	15 (47)
Ratnagiri	11 (23)	12 (60)

(Values in paranthesis indicate the rate of downward movement)

Similar analysis were carried out for 18°C isotherm, which represent the lower thermocline (Fig.3.6 and Table 3.1). During upwelling periods this isotherm is observed at its deepest depth (146m) in April-May which shoals to 103m in July at a rate of 17m off Cape Comorin. The corresponding values are 21m (183m in February to to 66m during

July-August), 15m (175m in March to 86m in September) and 12m (198m in March to 100m in November) off Cochin, Kasargod and Ratnagiri respectively. The downward movement of 18°C isotherm is 31m (113m in September to 190m during November-December), 72m (90m in September to 198m during October-November), 47m (106m during October-November to 176m in December) and 60m (100m during October-November to 190m in December) respectively off Cape Comorin, Cochin, Kasargod and Ratnagiri.

This suggests that rate of downward movements of isotherms in the thermocline is about 2 to 5 times faster than that of upward movements. Moreover, the rate of upward movements are more in the upper thermocline (30m per month for 23°C isotherm) compared to the lower thermocline (17m per month for 18°C isotherm). The reasons for the low rate of upward movement in the lower thermocline is discussed in section 3.4. However, during the periods of sinking, except off Cochin and Cape, the rate of downward movements are more in the lower thermocline. Moreover, the rate of downward movement is appreciably higher off Cochin compared to any other locations along the west coast of India.

3.6 T-S CHARACTERISTICS WITHIN THE THERMOCLINE OFF THE WEST COAST OF INDIA

The thermocline characteristics in the Arabian Sea is influenced by the presence of various watermasses during different times of the year (Wyrтки, 1971; Darbyshire, 1967; Sastry and D'Souza, 1972). Individual hydrographic data available off the west coast of India are utilised to map the T-S diagrams (Fig. 3.7) in order to identify some of the major watermasses in the thermocline and their monthly

evolution. The T-S plots show minimum scatter during May-June and September-October while relatively larger scatter is noticed during the rest of the year suggesting the presence of a number of watermasses having different T-S characteristics.

Prior to the onset of monsoon (May), salinity within the thermocline is between 35-36.25 PSU. The minimum scatter

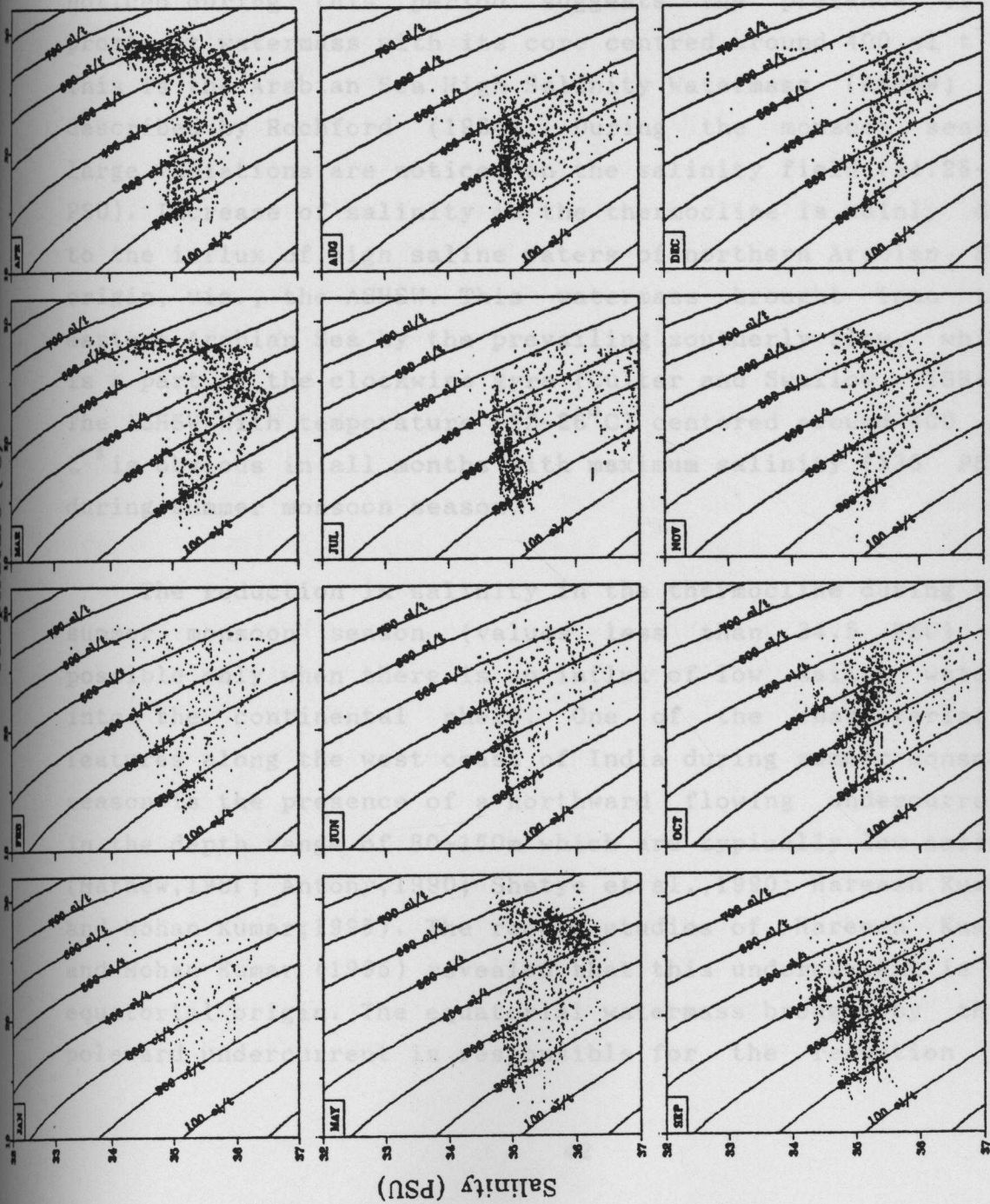


Fig. 3.7 T-S Characteristics within the thermocline for coastal waters (depth < 200m)

evolution. The T-S plots show minimum scatter during May-June and September-October while relatively larger scatter is noticed during the rest of the year suggesting the presence of a number of watermasses having different T-S characteristics.

Prior to the onset of monsoon (May), salinity within the thermocline is between 35-36.25 PSU. The minimum scatter noticed during this period suggests the presence of a prominent watermass with its core centred around 400 cl t^{-1} . This is the Arabian Sea High Salinity Watermass (ASHSW) as described by Rochford (1964). During the monsoon season large variations are noticed in the salinity field (34.25-37 PSU). Increase of salinity in the thermocline is mainly due to the influx of high saline waters of northern Arabian Sea origin, viz., the ASHSW. This watermass brought into the eastern Arabian Sea by the prevailing southerly flow, which is a part of the clockwise gyre (Culter and Swallow, 1984). The ASHSW with temperature ($22-26^{\circ}\text{C}$) centered around 400 cl t^{-1} is obvious in all months with maximum salinity ($>36 \text{ PSU}$) during summer monsoon season.

The reduction in salinity in the thermocline during the summer monsoon season (values less than 34.5 PSU) is possible only when there is an influx of low saline waters into the continental shelf. One of the characteristic features along the west coast of India during summer monsoon season is the presence of a northward flowing undercurrent in the depth range of 80-150m which are typically low saline (Mathew, 1981; Antony, 1990; Shetye et al., 1990; Hareesh Kumar and Mohan Kumar; 1995). The recent studies of Hareesh Kumar and Mohan Kumar (1995) revealed that this undercurrent is of equatorial origin. The equatorial watermass brought by this poleward undercurrent is responsible for the reduction in

salinity in the thermocline during summer monsoon season. The existence of high saline ASHSW over the low saline equatorial Indian Ocean watermass produce large scatter in the T-S diagram during summer monsoon.

Several studies have reported the influx of Bay of Bengal/Equatorial Indian Ocean water (above 500 cl t⁻¹) into the shelf regions of the west coast of India during winter (Darbyshire, 1967; Wyrтки, 1971; Pankajakshan and Ramaraju, 1987; Hareesh Kumar, 1994). The T-S characteristics above 500 cl t⁻¹ indicate uniform temperature (28°C) and rapidly decreasing salinity (35-33.5 PSU in March). However, this reduction in salinity is less compared to the values (35-32 PSU) reported by Hareesh Kumar (1994) for the entire water column. This suggests that the influence of Bay of Bengal/Equatorial Indian Ocean water is limited to the upper thermocline (with temperature above 27°C).

3.7 THERMOCLINE CHARACTERISTICS IN THE COASTAL REGIONS

The available temperature data in the coastal region (depth <200m) along the west coast of India (6° to 24°N) averaged in 0.25 x 0.25 degree square are utilised for this investigation. The thermocline characteristics, viz top of the thermocline, its average temperature and average gradient are presented in Figs.(3.(8-10)) to highlight its spatio-temporal variations.

Topography of the thermocline (Fig.3.8) exhibits large variations from December to March. Top of the thermocline ascends from February onwards (100m in February to 50m in March) in the lower latitudes (at 9°N) suggesting the beginning of upwelling. The thermocline is quite shallow (<50m) along the entire west coast of India during the

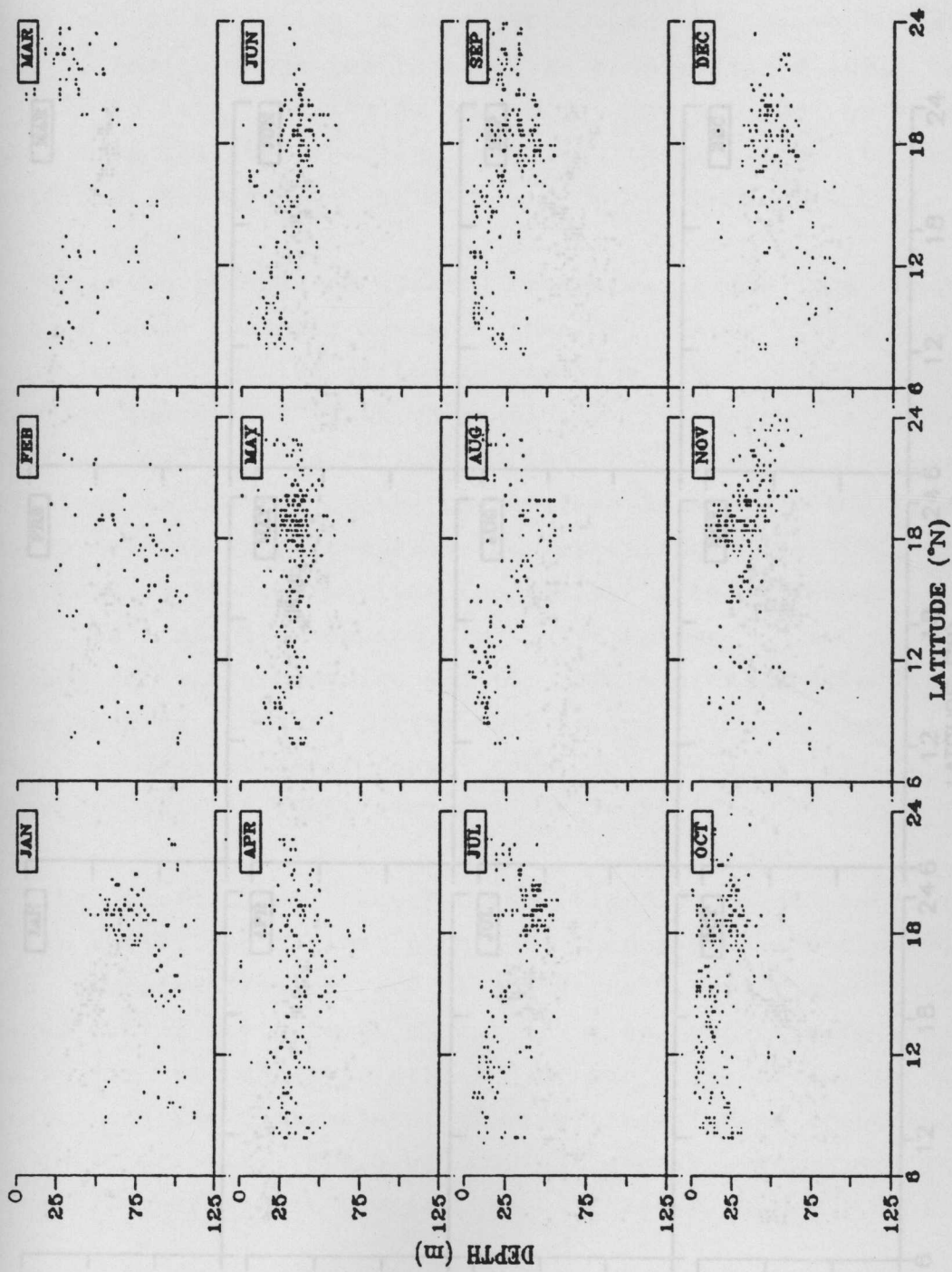


Fig. 3.8 Zonal distribution of thermocline top for coastal waters
(depth < 200m)

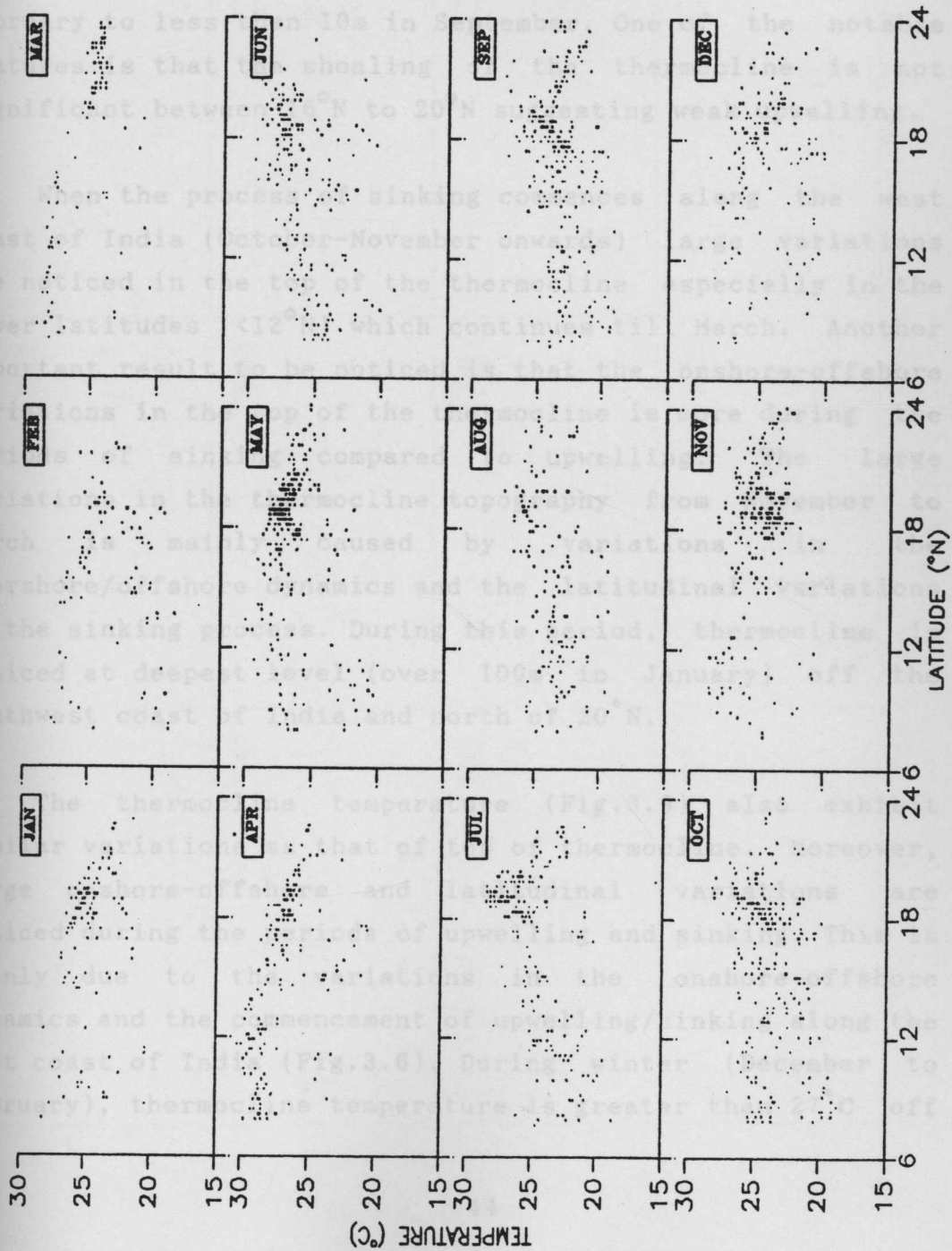


Fig. 3.9 Zonal distribution of thermocline temperature for coastal waters (depth < 200m)

pre-monsoon (April-May) and monsoon (June-September) seasons. The shallow thermocline during the pre-monsoon season is mainly caused by the accumulation of heat in the surface layers (Hastenrath and Lamb, 1979) which stabilises the water column. However, during the summer monsoon season upwelling is the prime factor controlling its variability. The effect of upwelling is more pronounced off the southwest coast of India, where the thermocline shoals from $\approx 100\text{m}$ in February to less than 10m in September. One of the notable features is that the shoaling of the thermocline is not significant between 16°N to 20°N suggesting weak upwelling.

When the process of sinking commences along the west coast of India (October-November onwards) large variations are noticed in the top of the thermocline especially in the lower latitudes ($<12^{\circ}\text{N}$) which continues till March. Another important result to be noticed is that the onshore-offshore variations in the top of the thermocline is more during the periods of sinking compared to upwelling. The large variations in the thermocline topography from November to March is mainly caused by variations in the nearshore/offshore dynamics and the latitudinal variations in the sinking process. During this period, thermocline is noticed at deepest level (over 100m in January) off the southwest coast of India and north of 20°N .

The thermocline temperature (Fig.3.9) also exhibit similar variations as that of top of thermocline. Moreover, large onshore-offshore and latitudinal variations are noticed during the periods of upwelling and sinking. This is mainly due to the variations in the onshore-offshore dynamics and the commencement of upwelling/sinking along the west coast of India (Fig.3.6). During winter (December to February), thermocline temperature is greater than 27°C off

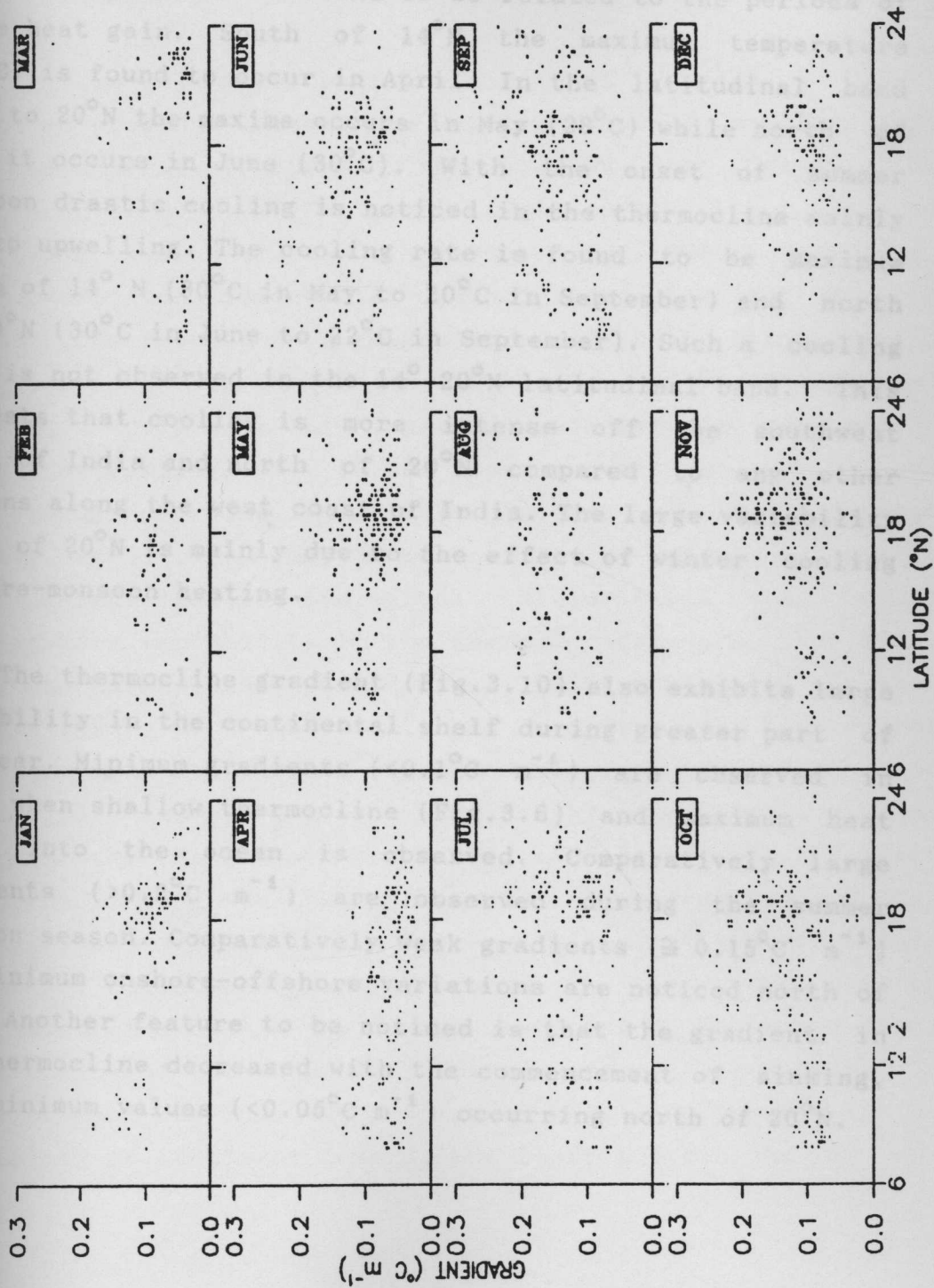


Fig. 3.10 Zonal distribution of thermocline gradient for coastal waters (depth < 200m)

the southwest coast of India and decreases towards north ($\cong 23^{\circ}\text{C}$ north of 20°N). In association with large heat input into the ocean during the pre-monsoon period (Hastenrath and Lamb, 1979), temperature in the thermocline increases. If we closely examine the temperature pattern, occurrence of maximum temperature is found to be related to the periods of large heat gain. South of 14°N the maximum temperature (30°C) is found to occur in April. In the latitudinal band 14°N to 20°N the maxima occurs in May (28°C) while north of 20°N it occurs in June (30°C). With the onset of summer monsoon drastic cooling is noticed in the thermocline mainly due to upwelling. The cooling rate is found to be maximum south of 14°N (30°C in May to 20°C in September) and north of 20°N (30°C in June to 22°C in September). Such a cooling rate is not observed in the 14° - 20°N latitudinal band. This suggests that cooling is more intense off the southwest coast of India and north of 20°N compared to any other regions along the west coast of India. The large variability north of 20°N is mainly due to the effect of winter cooling and pre-monsoon heating.

The thermocline gradient (Fig.3.10) also exhibits large variability in the continental shelf during greater part of the year. Minimum gradients ($<0.1^{\circ}\text{C m}^{-1}$) are observed in April when shallow thermocline (Fig.3.6) and maximum heat input into the ocean is observed. Comparatively large gradients ($>0.2^{\circ}\text{C m}^{-1}$) are observed during the summer monsoon season. Comparatively weak gradients ($\cong 0.15^{\circ}\text{C m}^{-1}$) and minimum onshore-offshore variations are noticed north of 20°N . Another feature to be noticed is that the gradient in the thermocline decreased with the commencement of sinking, with minimum values ($<0.05^{\circ}\text{C m}^{-1}$) occurring north of 20°N .

CHAPTER IV

SHORT-TERM VARIABILITY OF THERMOCLINE CHARACTERISTICS

4.1. INTRODUCTION

It is well known that the onset and progress of summer monsoon produces large scale spatio-temporal modifications in the thermal structure of the Arabian Sea (Wyrski, 1971; Robinson et al., 1979; Molinari, 1983; Shetye 1986; Rao et al., 1989; Rao et al., 1990; Hareesh Kumar, 1994). Generally, the pre-monsoon season is characterised by fair weather conditions resulting in accumulation of heat with varying magnitudes across the basin. However, due to occasional thunder squall activities, marked variations are noticed in the meteorological (Sikka and Grossman, 1980) and thermohaline fields (Rao, 1987; Rao et al., 1993; Hareesh Kumar, 1994) on a synoptic scale. Active monsoonal spells and associated meteorological disturbances can cause short-term variability in the thermal structure (Rao, 1986; Rao and Mathew, 1990; Joseph et al., 1990; Murthy and Hareesh Kumar, 1991). With the onset and progress of the summer monsoon, intense air-sea exchange processes (Hastenrath and Lamb, 1979) and convergence induced by the negative wind stress curl (Hastenrath and Lamb, 1979; Bauer et al., 1991) deepens ($\approx 100\text{m}$) the thermocline in the central Arabian Sea (Sastry and D'Souza, 1970; Hastenrath and Greischar, 1989). However, significant warming occurs in the upper portion of thermocline mainly due to the deepening of the mixed layer and mixing of the subsurface waters with surface waters. In the coastal regions, the process of upwelling results in the shoaling of isotherms towards the coast and cooling of the

water column (Warren et al., 1986; Swallow and Bruce, 1988; Schott, 1983; Mathew, 1981; Shetye et al., 1991).

Prior to the conduct of summer monsoon experiments no systematic time series measurements were made to study the short term variability of thermal structure in the Arabian Sea. During these experimental programmes a systematic attempt was made to collect vertical temperature and salinity data at selected locations in the Arabian Sea. Although the data sets were collected at different locations over short duration, they provide important insight into the thermocline variability.

In the Arabian Sea, several studies have been carried out to understand the time variation of the thermocline and its cause, i.e. factors (Rao, 1986; McCreary and Gouveia, 1989; Joseph et al., 1990; Ramesh Babu and Mathew, 1990; Shetye et al., 1991; Mohan Kumar et al., 1995; Hareesh Kumar, 1994; Hareesh Kumar and Mohankumar, 1995). However, the evolution of the thermocline characteristics viz, top of the thermocline, thickness, gradient, mixing processes, oscillations is not adequately described or understood. In this chapter, the short term variability in the thermocline characteristics is studied utilising the time series data sets collected from selected locations in the Arabian Sea during the pre-monsoon and monsoon phases of the summer monsoon.

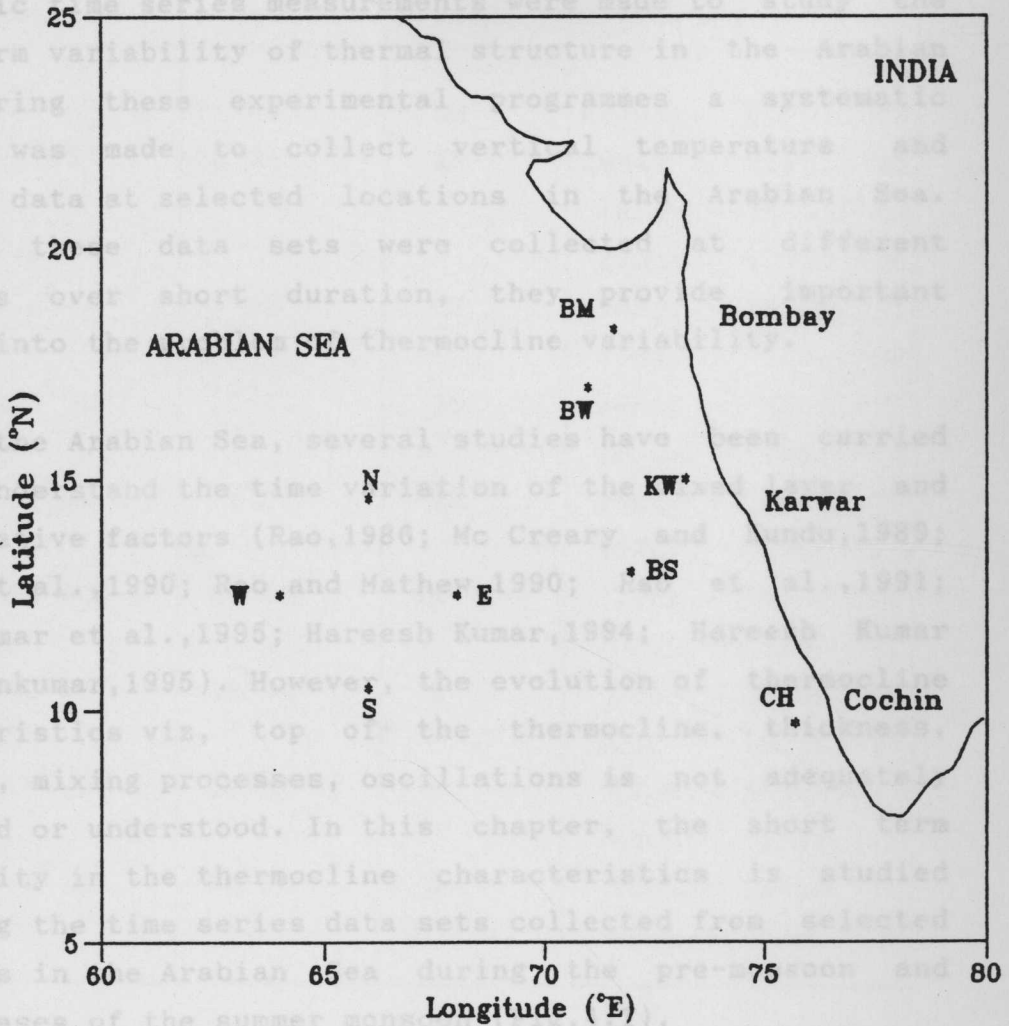


Fig. 4.1 Station location map of time series observations

4.2. DATA

Most of the data sets utilised for this study correspond to open ocean conditions of the Arabian Sea were collected during NONSOON-77 and NONEX-79 field experimental programmes. In addition, data sets collected in the coastal zones off Bombay, Karwar and Cochin are utilised. The

water column (Warren et al.,1966; Swallow and Bruce,1966; Schott,1983; Mathew,1981; Shetye et al.,1991).

Prior to the conduct of summer monsoon experiments no systematic time series measurements were made to study the short term variability of thermal structure in the Arabian Sea. During these experimental programmes a systematic attempt was made to collect vertical temperature and salinity data at selected locations in the Arabian Sea. Although these data sets were collected at different locations over short duration, they provide important insight into the problem of thermocline variability.

In the Arabian Sea, several studies have been carried out to understand the time variation of the mixed layer and its causative factors (Rao,1986; Mc Creary and Kundu,1989; Joseph et al.,1990; Rao and Mathew,1990; Rao et al.,1991; Mohan Kumar et al.,1995; Hareesh Kumar,1994; Hareesh Kumar and Mohankumar,1995). However, the evolution of thermocline characteristics viz, top of the thermocline, thickness, gradient, mixing processes, oscillations is not adequately discribed or understood. In this chapter, the short term variability in the thermocline characteristics is studied utilising the time series data sets collected from selected locations in the Arabian Sea during the pre-monsoon and onset phases of the summer monsoon (Fig.4.1).

4.2. DATA

Most of the data sets utilised for this study correspond to open ocean conditions of the Arabian Sea were collected during MONSOON-77 and MONEX-79 field experimental programmes. In addition, data sets collected in the coastal zones off Bombay, Karwar and Cochin are utilised. The

Table 4.1
Station location, Symbol and observation period

Station location		Station Symbol	Observation Period
Latitude	Longitude		
18°15'	71°35'	BM	28Jun.- 01Jul.'88
14°45'	73°35'	KW	28May - 01Jul.'89 18Sep.- 25Sep.'89 29Oct.- 10Nov.'86
09°44'	75°42'	CH	10Apr.- 17Apr.'91 23May - 3Jun.'92
13°00'	72°00'	BS	26May - 7Jun.'77 26Jun.- 14Jul.'77
17°00'	71°00'	BW	26May - 7Jun.'77 26Jun.- 13Jul.'77
14°30'	66°00'	N	7Jun.- 19Jun.'77 30Jun.- 15Jul.'77
12°30'	68°00'	E	7Jun.- 19Jun.'77 30Jun.- 15Jul.'77
10°30'	66°00'	S	7Jun.- 19Jun.'77 30Jun.- 15Jul.'77
12°30'	64°00'	W	7Jun.- 19Jun.'77 30Jun.- 15Jul.'77

period, April-May represents pre-onset and June to September represents active phases of the summer monsoon. The station locations (Fig.4.1) are designated as N, E, S and W correspond to the four corners of the USSR polygon occupied in the central Arabian Sea during 1977 and BW and BS

represents two Indian ship locations in the eastern Arabian Sea during MONSOON-77. BM, KW and CH are the three coastal stations off Bombay, Karwar and Cochin respectively. Station locations, symbols and observational periods are presented in Table 4.1. From these locations time series of the vertical profiles of temperature were collected at one/three/six hourly sampling interval. To study the role of mixing process in the thermocline region the subsurface currents obtained from selected depth levels by deploying Aanderaa RCM4 and RCM7 current meters at CH, KW, BM are also utilised.

4.3. RESULTS AND DISCUSSION

4.3.1 DEPTH-TIME SECTIONS OF THERMAL STRUCTURE

The depth-time sections of temperature presented in Fig.4.2 reveal the complex nature of spatio-temporal variability in the thermocline. One of the features that has to be noted is the occurrence of variable gradients and oscillatory nature in the thermocline. In the discussion, the depth-time sections of temperature for the coastal and deep stations are treated separately.

4.3.1.1 AT COASTAL STATIONS

The thermal structure off Bombay (Fig.4.2a) is characterised by a tri-layer structure with a sharp thermocline (2.5°C drop in 10m) sandwiched between upper (40m) and bottom (25m) isothermal layers. Formation of this feature can be explained in terms of air-sea interaction process. During winter, the thermal structure in the continental shelf off Bombay is characterised by deep isothermal layers ($\approx 80\text{m}$) with temperature $\approx 26.5^{\circ}\text{C}$ (Joseph

Fig. 4.2 Depth-time sections of temperature at (a) BM (b) KW (c) CH representing shallow water (depth < 200m) ($^{\circ}\text{C}$)

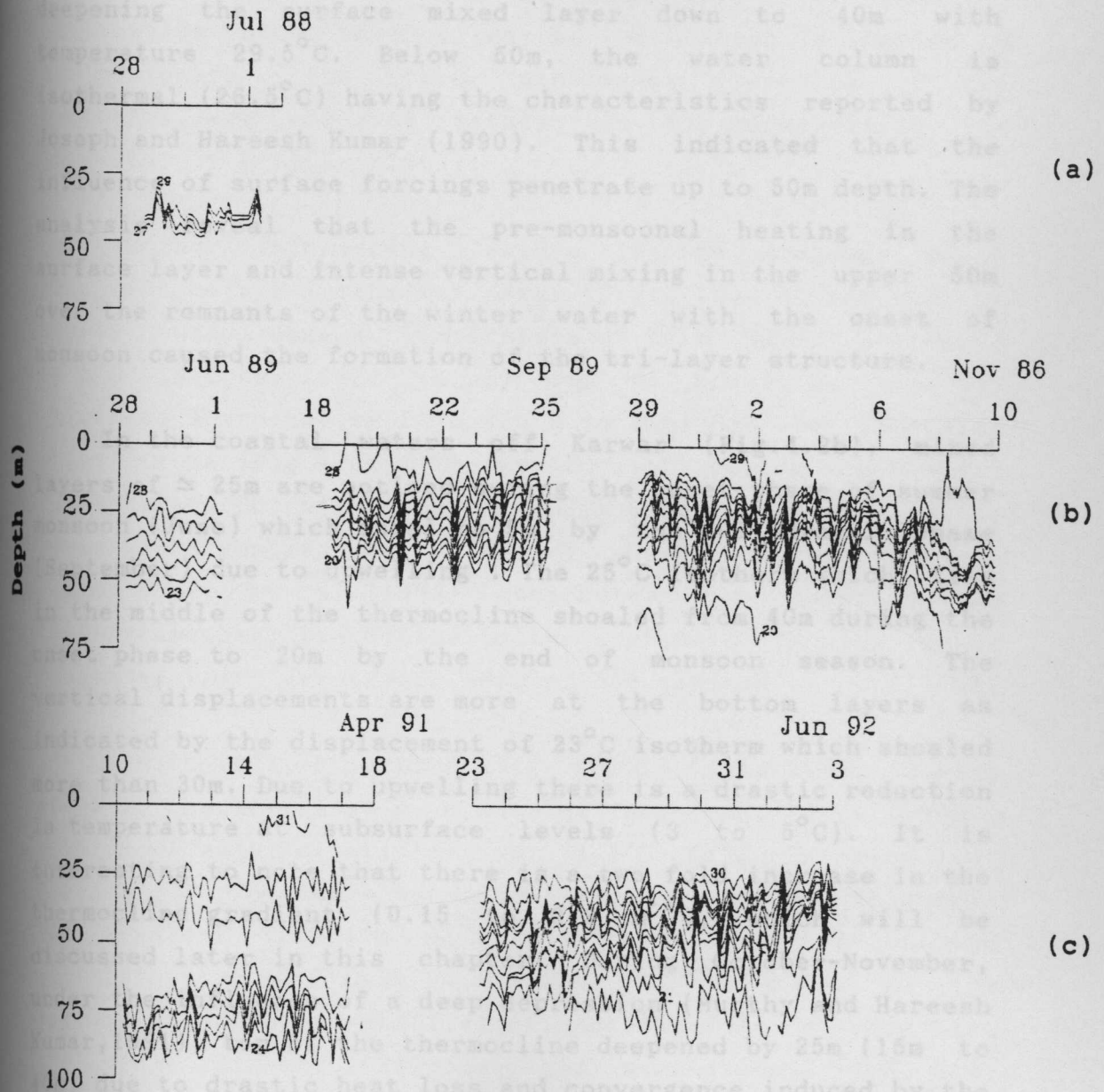


Fig. 4.2 Depth-time sections of temperature at (a) BM (b) KW (c) CH representing shallow water (depth <200m) ($^{\circ}\text{C}$)

displacement (October-November) in the thermocline revealed
and Hareesh Kumar,1990). During the pre-monsoon period, climatological studies of Rao et al.(1990) reported a warming of 4°C in the surface layers. Intense vertical mixing (Hastenrath and Lamb,1979) of the surface warmer waters with subsurface cooler waters during the summer monsoon caused the re-distribution of heat, thereby deepening the surface mixed layer down to 40m with temperature 29.5°C . Below 50m, the water column is isothermal (26.5°C) having the characteristics reported by Joseph and Hareesh Kumar (1990). This indicated that the influence of surface forcings penetrate up to 50m depth. The analysis reveal that the pre-monsoonal heating in the surface layer and intense vertical mixing in the upper 50m over the remnants of the winter water with the onset of monsoon caused the formation of the tri-layer structure.

In the coastal waters off Karwar (Fig.4.2b), mixed layers of $\approx 25\text{m}$ are noticed during the onset phase of summer monsoon (June) which shoal to 5m by the withdrawal phase (September) due to upwelling . The 25°C isotherm which lies in the middle of the thermocline shoaled from 40m during the onset phase to 20m by the end of monsoon season. The vertical displacements are more at the bottom layers as indicated by the displacement of 23°C isotherm which shoaled more than 30m. Due to upwelling there is a drastic reduction in temperature at subsurface levels (3 to 5°C). It is interesting to note that there is a two fold increase in the thermocline gradient (0.15 to 0.3 m^{-1}), which will be discussed later in this chapter. During October-November, under the influence of a deep depression (Murthy and Hareesh Kumar,1991), top of the thermocline deepened by 25m (15m to 40m) due to drastic heat loss and convergence induced by the surface wind stress curl (Murthy and Hareesh Kumar,1991). Fast Fourier Transform (FFT) analysis of isotherm

displacement (October-November) in the thermocline revealed oscillations with semi-diurnal (12 hrs), diurnal (24 hrs) and inertial (46 hrs) periodicities. The oscillation with inertial periodicity is caused by the distant storm centred 360km southwest of observational station and caused vertical displacement of 15-20m in the isotherms. Pollard (1970) also observed similar conditions during the passage of storm and attributed the wind field as the main source of inertial oscillation in the thermocline. As the station is located at the periphery of the storm, continuous deepening of the isotherms are observed mainly due to downwelling as suggested by Leipper (1967).

Another interesting feature is the presence of a prominent bottom isothermal layer (Fig.4.2b). By the end of summer monsoon season, temperature of this layer decreased by 3°C (23°C to 20°C) mainly due to upwelling and its thickness increased by 15 m (10 m to 25m) due to increased shear mixing (Fig.4.6b). The presence of bottom isothermal layer during October-November though with an increase in its temperature compared to withdrawl phase suggest sinking. Mohan Kumar et al.(1995) attributed the increase in temperature near the bottom to the northward flowing under currents, which are typical during the periods of upwelling.

The thermal structure off Cochin (Fig.4.2c) during April is characterised by a shallow isothermal layer ($\cong 20\text{m}$), a layer of weak stratification (1.5°C fall in 20m i.e. $0.075^{\circ}\text{C m}^{-1}$), a quasi-homogeneous layer (5 to 20m thickness and gradient $< 0.025^{\circ}\text{C m}^{-1}$) and a layer of strong stratification (5°C fall in 30m i.e. $0.17^{\circ}\text{C m}^{-1}$). In the regions of strong stratification, oscillations of inertial (79 hrs), diurnal (24 hrs) and semi-diurnal (12 hrs) periodicities are noticed, due to which the isotherms are

displaced by $\approx 5-15\text{m}$ in the vertical. The layer of weak stratification is thought to be the result of deep mixed layer during winter followed by surface heating (Hareesh Kumar and Mohan Kumar, 1995) during the pre-monsoon season. Thickness of the quasi-homogeneous layer decrease from 30m to 5m between 10 and 14 April and increase thereafter. By May, this quasi-homogeneous layer disappear and the thermocline becomes more stratified ($0.15^{\circ}\text{C.m}^{-1}$). Moreover there is an upward displacement of isotherms in the thermocline during this period. For instance, in the thermocline the 25°C isotherm, which was at 85m on 17 April, shoaled to 35m by 3 June, with an average upward movement of 1.1 m.day^{-1} . This upward movement of isotherms are mainly due to the process of upwelling, results in cooling of $\approx 0.8^{\circ}\text{C}$ at the surface and 4.5°C at the bottom, with maximum cooling in the of 6°C at 60m.

4.3.1.2 AT DEEP STATIONS

In the eastern Arabian Sea (BS and BW), intense solar heating during the pre-monsoon phase (Rao et al., 1990) resulting in the formation of near surface ($<20\text{m}$) thermocline (Fig.4.2(d,e)). The enhanced vertical mixing during the summer monsoon season deepens the thermocline to below 50m. However, the effect of upwelling is noticed within the thermocline at both locations as evident from the upward displacement of 24°C isotherm which shoaled by 25m at BS (90m to 65m) and 20m at BW (80m to 60m). Several short period oscillations are also noticed in the thermocline in both the phases.

Fig. 4.2 Depth-time sections of temperature at (d) BS (e) BW

The observed thermal structure at the polygon stations (Figs.4.2(f-i)) in the central Arabian Sea is significantly different from the stations in the coastal regions in many

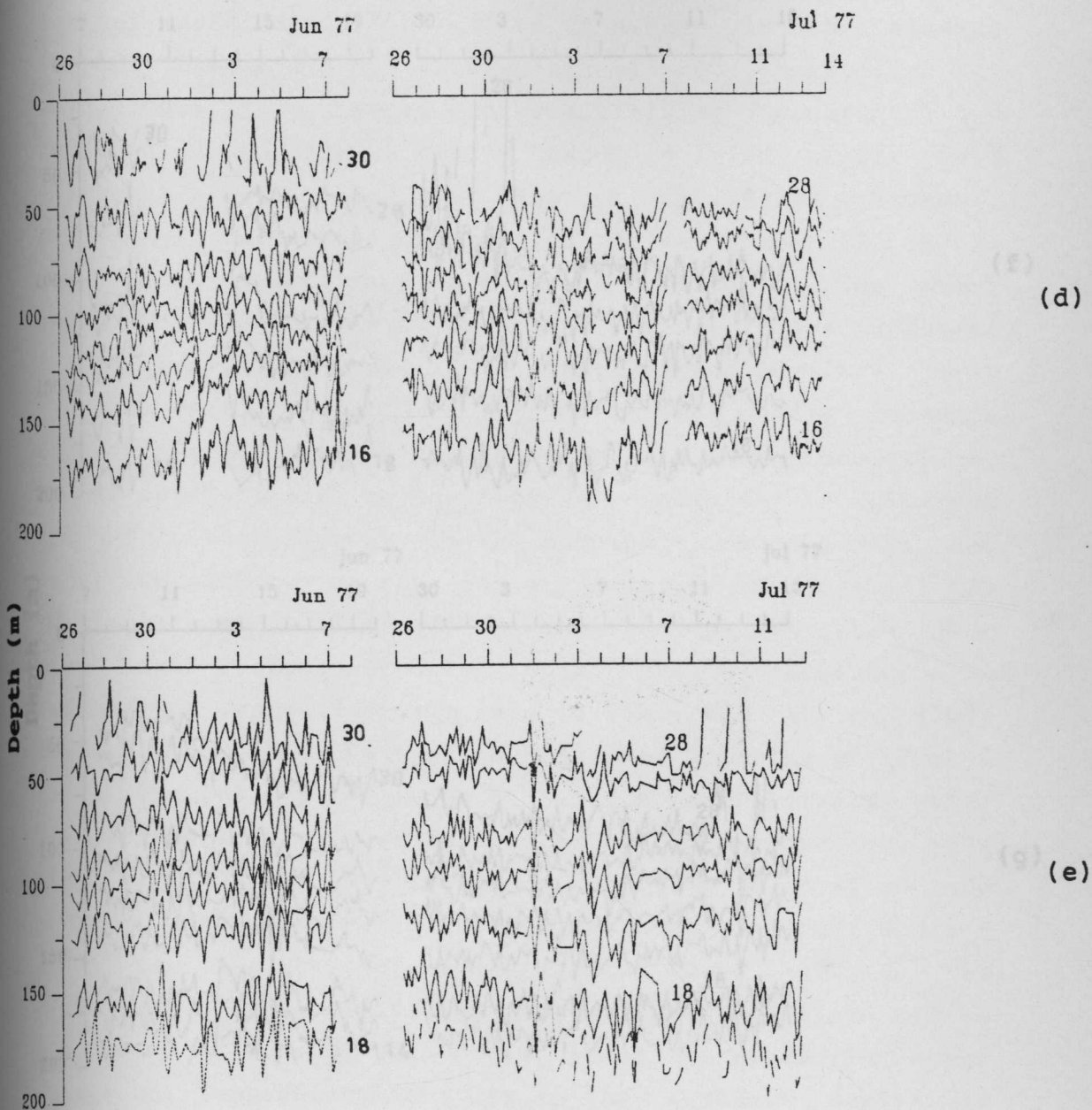
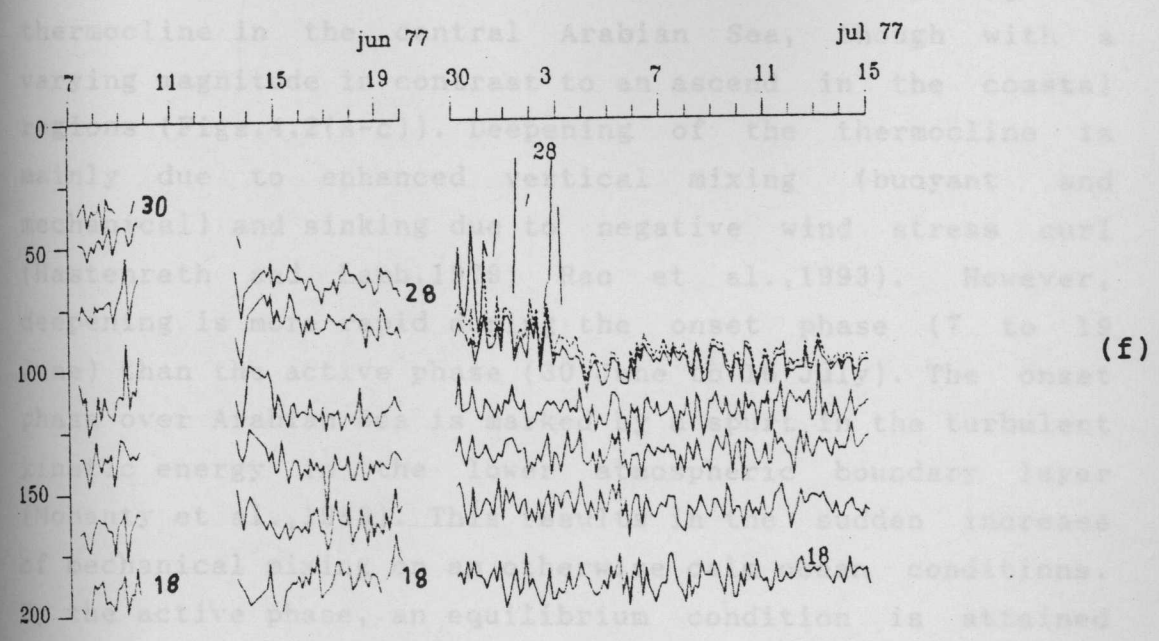
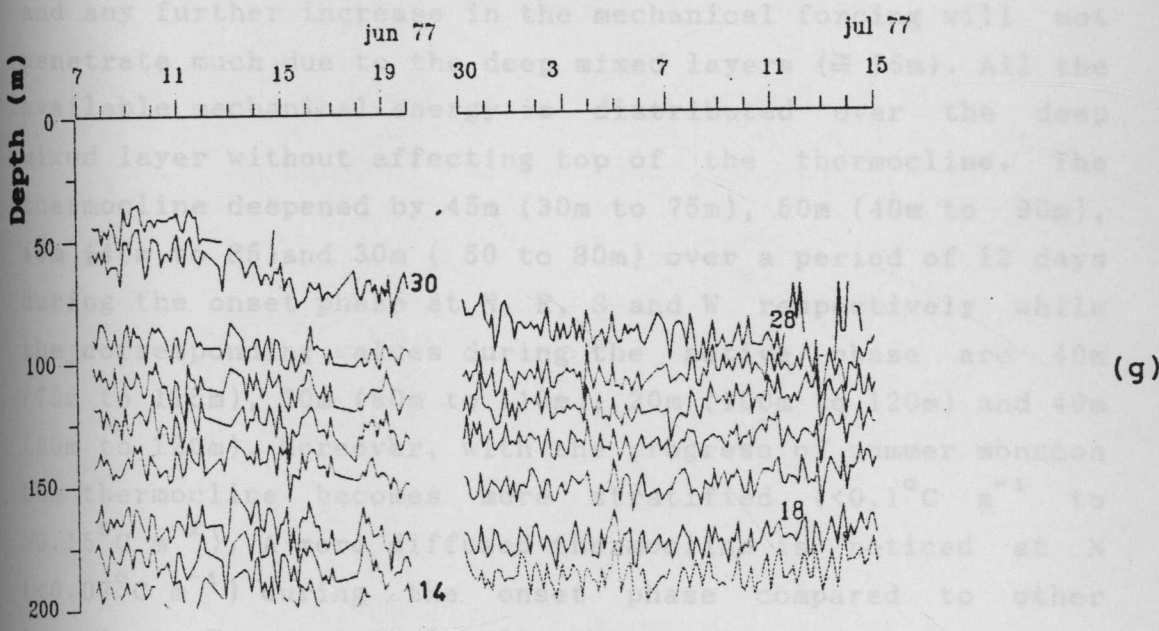


Fig. 4.2 Depth-time sections of temperature at (d) BS (e) BW representing deep water (depth >1000m) ($^{\circ}\text{C}$)



(f)



(g)

Fig. 4.2 Depth-time sections of temperature at (f) N (g) E representing deep water (depth >1000m) (°C)

respects. A noteworthy feature is the deepening of thermocline in the central Arabian Sea, though with a varying magnitude in contrast to an ascend in the coastal regions (Figs.4.2(a-c)). Deepening of the thermocline is mainly due to enhanced vertical mixing (buoyant and mechanical) and sinking due to negative wind stress curl (Hastenrath and Lamb,1979; Rao et al.,1993). However, deepening is more rapid during the onset phase (7 to 19 June) than the active phase (30 June to 16 July). The onset phase over Arabian Sea is marked by a spurt in the turbulent kinetic energy in the lower atmospheric boundary layer (Mohanty et al.,1983). This results in the sudden increase of mechanical mixing on an otherwise calm ocean conditions. By the active phase, an equilibrium condition is attained and any further increase in the mechanical forcing will not penetrate much due to the deep mixed layers ($\approx 75\text{m}$). All the available mechanical energy is distributed over the deep mixed layer without affecting top of the thermocline. The thermocline deepened by 45m (30m to 75m), 50m (40m to 90m), 45m (40m to 85)and 30m (50 to 80m) over a period of 12 days during the onset phase at N, E, S and W respectively while the corresponding values during the active phase are 40m (75m to 115m), 30m (80m to 110m), 20m (100m to 120m) and 40m (80m to 120m). Moreover, with the progress of summer monsoon the thermocline becomes more stratified ($<0.1^\circ\text{C m}^{-1}$ to $>0.15^\circ\text{C m}^{-1}$). A more diffused thermocline is noticed at N ($<0.07^\circ\text{C m}^{-1}$) during the onset phase compared to other locations. Temporal variability in the isotherm depths in the thermocline shows oscillatory pattern caused by propagating internal waves and eddy fields etc. (Duing,1972; Swallow et al.,1983).

4.3.2 SHORT-TERM VARIATIONS OF THERMOCLINE CHARACTERISTICS

From the analysis of time series of thermal structure at selected location, it is found that there are significant variations in the thermocline characteristics. In the present study, the characteristics of the thermocline are studied via, top of thermocline, thickness, gradient, mixing in the thermocline and oscillations in the thermocline are

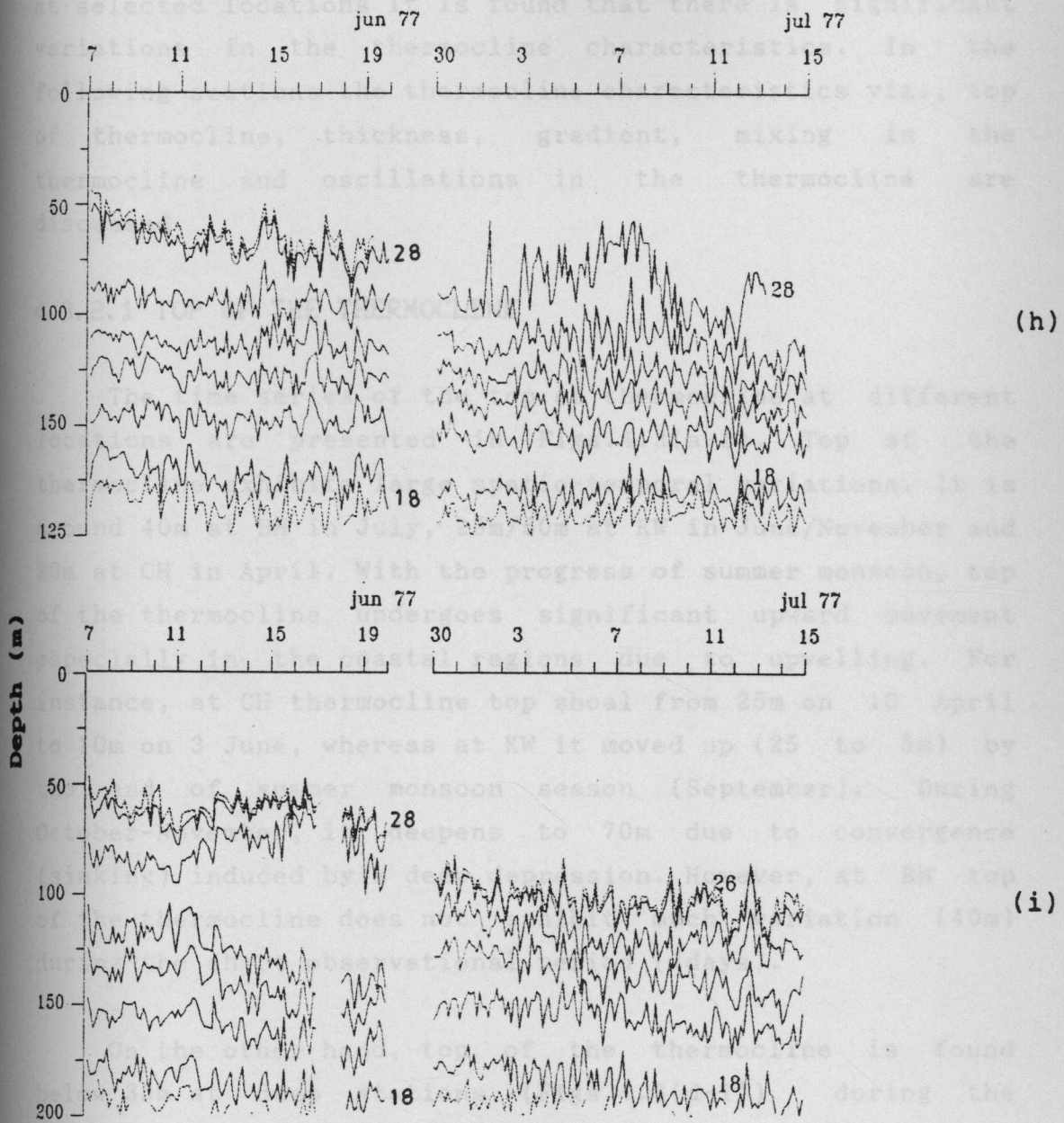


Fig. 4.2 Depth-time sections of temperature at (h) S (i) W representing deep water (depth >1000m)(°C)

4.3.2 SHORT-TERM VARIATIONS OF THERMOCLINE CHARACTERISTICS

From the analysis of time series of thermal structure at selected locations it is found that there is significant variations in the thermocline characteristics. In the following sections the thermocline characteristics viz., top of thermocline, thickness, gradient, mixing in the thermocline and oscillations in the thermocline are discussed.

4.3.2.1 TOP OF THE THERMOCLINE

The time series of the top of thermocline at different locations are presented in Figs.4.3(a-i). Top of the thermocline exhibits large spatio-temporal variations. It is around 40m at BM in July, 25m/50m at KW in June/November and 20m at CH in April. With the progress of summer monsoon, top of the thermocline undergoes significant upward movement especially in the coastal regions due to upwelling. For instance, at CH thermocline top shoal from 25m on 10 April to 10m on 3 June, whereas at KW it moved up (25 to 5m) by the end of summer monsoon season (September). During October-November, it deepens to 70m due to convergence (sinking) induced by a deep depression. However, at BM top of the thermocline does not exhibit much variation (40m) during the short observational period (4days).

On the other hand, top of the thermocline is found below 35m at deep stations (Figs.4.3(d-i)) during the entire observational period. In the central (Figs.4.3(f-i)) and at the two stations in the eastern Arabian Sea (Figs.4.3(d&e)), it continuously deepened from 40-75m and 35-120m respectively due to intense vertical mixing (Hastenrath and Lamb,1979) and sinking with the onset and

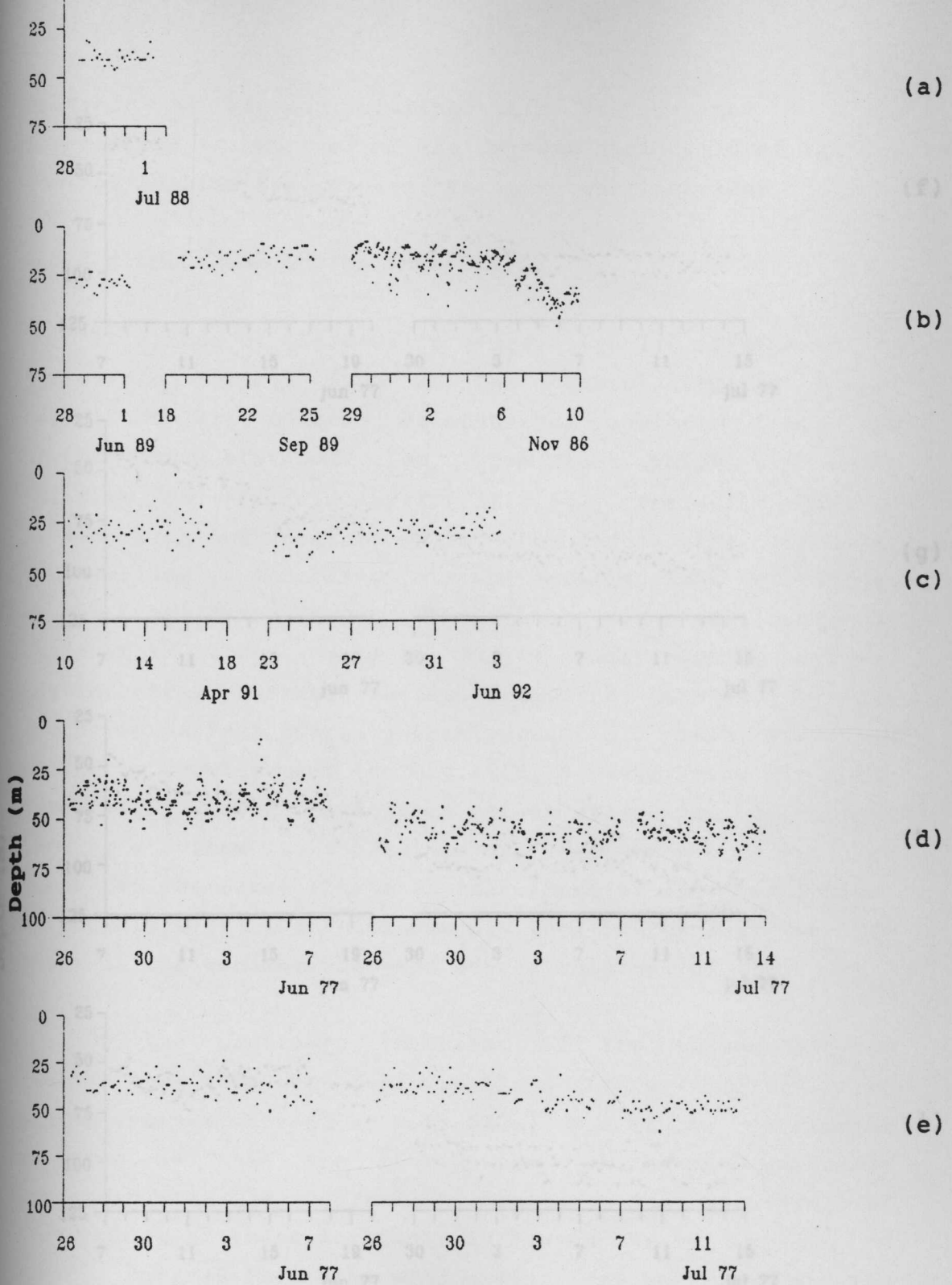


Fig.4.3 Time series of thermocline top at (a) BM (b) KW
(c) CH (d) BS (e) BW

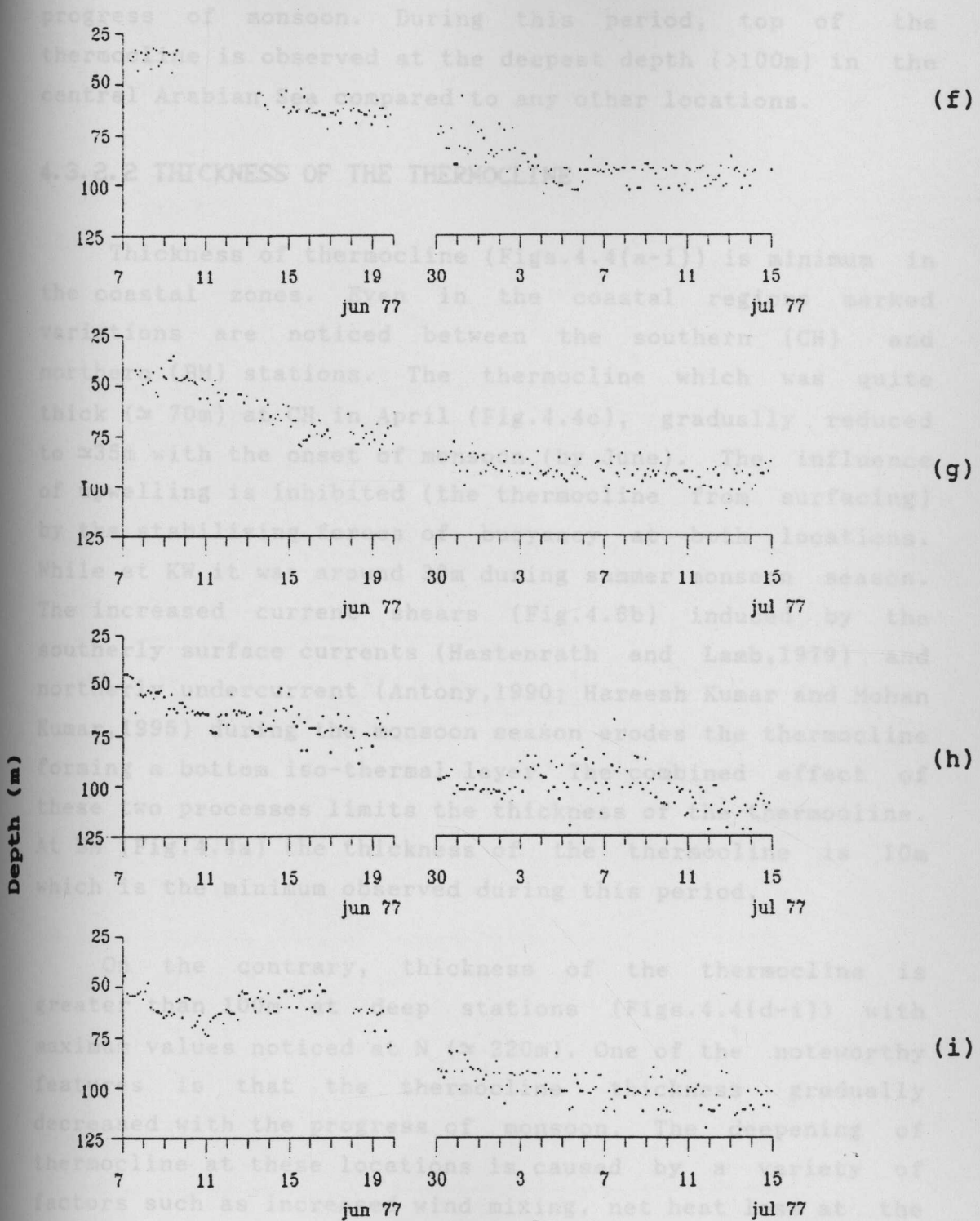


Fig.4.3 Time series of thermocline top at (f) N (g) E
(h) S (i) W

progress of monsoon. During this period, top of the thermocline is observed at the deepest depth (>100m) in the central Arabian Sea compared to any other locations.

4.3.2.2 THICKNESS OF THE THERMOCLINE

Thickness of thermocline (Figs.4.4(a-i)) is minimum in the coastal zones. Even in the coastal regions marked variations are noticed between the southern (CH) and northern (BM) stations. The thermocline which was quite thick ($\approx 70\text{m}$) at CH in April (Fig.4.4c), gradually reduced to $\approx 35\text{m}$ with the onset of monsoon (by June). The influence of upwelling is inhibited (the thermocline from surfacing) by the stabilising forces of buoyancy at both locations. While at KW it was around 30m during summer monsoon season. The increased current shears (Fig.4.6b) induced by the southerly surface currents (Hastenrath and Lamb,1979) and northerly undercurrent (Antony,1990; Hareesh Kumar and Mohan Kumar,1995) during the monsoon season erodes the thermocline forming a bottom iso-thermal layer. The combined effect of these two processes limits the thickness of the thermocline. At BM (Fig.4.4a) the thickness of the thermocline is 10m which is the minimum observed during this period.

On the contrary, thickness of the thermocline is greater than 100m at deep stations (Figs.4.4(d-i)) with maximum values noticed at N ($\approx 220\text{m}$). One of the noteworthy features is that the thermocline thickness gradually decreased with the progress of monsoon. The deepening of thermocline at these locations is caused by a variety of factors such as increased wind mixing, net heat loss at the surface, convergence due to negative wind stress curl (Hastenrath and Lamb, 1979) and entrainment at the bottom of mixed layer (Ramesh Babu and Sastry,1984). The convergence at

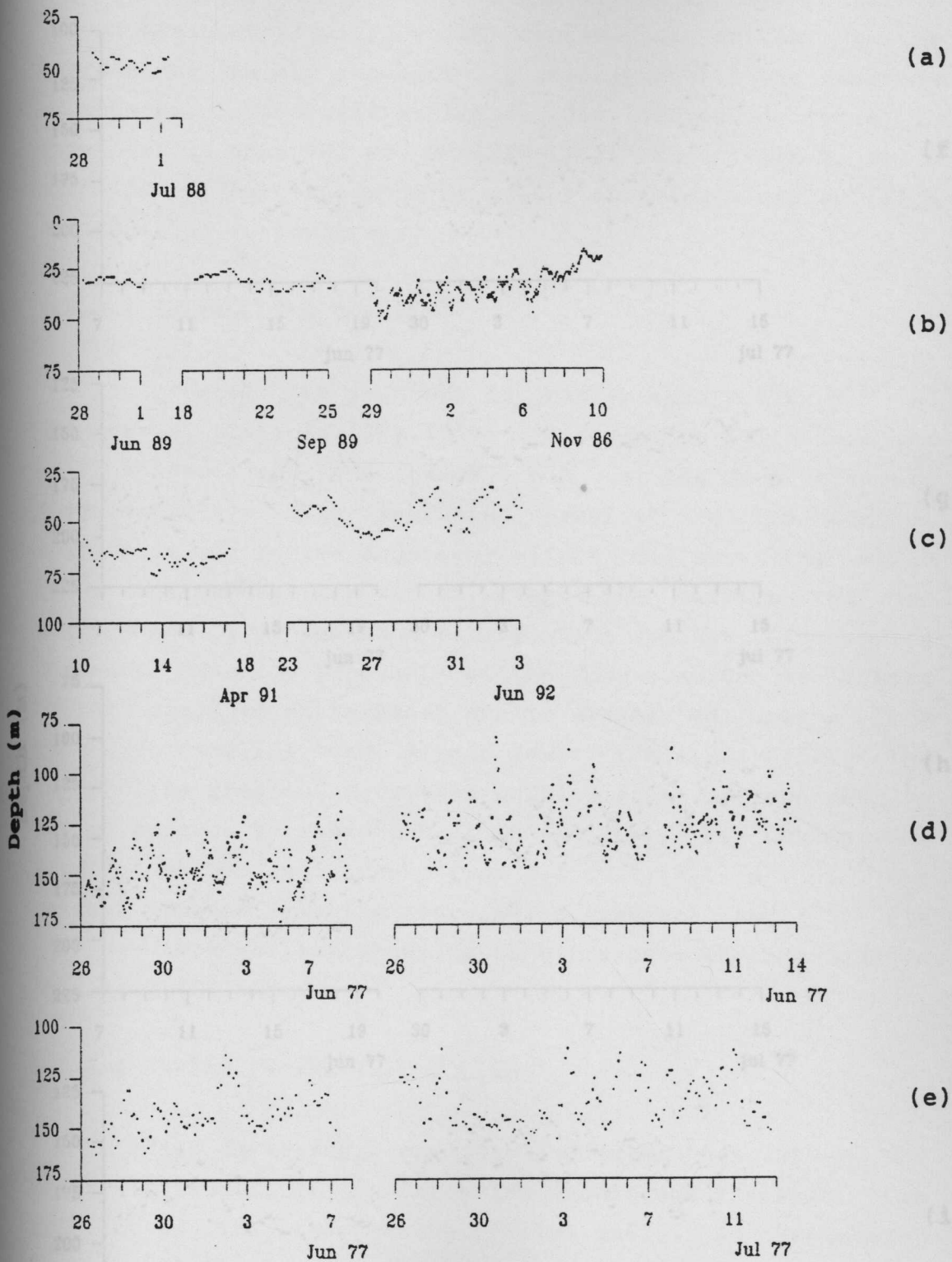


Fig.4.4 Time series of thermocline thickness at (a) BM (b) KW
 (c) CH (d) BS (e) BW

Fig.4.4 Time series of thermocline thickness at (a) N (b) E
 (c) S (d) W

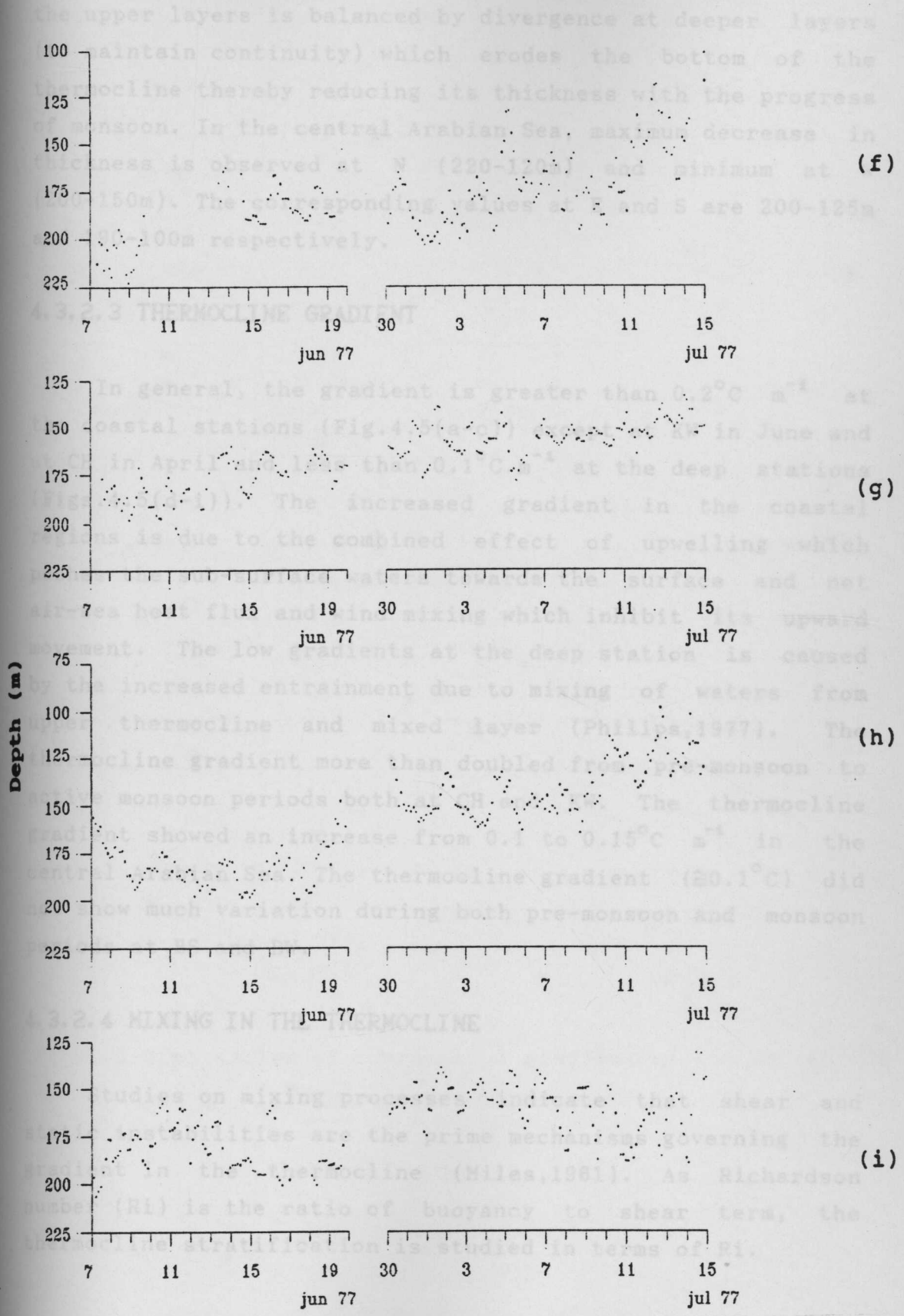


Fig.4.4 Time series of thermocline thickness at (f) N (g) E (h) S (i) W

the upper layers is balanced by divergence at deeper layers (to maintain continuity) which erodes the bottom of the thermocline thereby reducing its thickness with the progress of monsoon. In the central Arabian Sea, maximum decrease in thickness is observed at N (220-120m) and minimum at W (200-150m). The corresponding values at E and S are 200-125m and 190-100m respectively.

4.3.2.3 THERMOCLINE GRADIENT

In general, the gradient is greater than $0.2^{\circ}\text{C m}^{-1}$ at the coastal stations (Fig.4.5(a-c)) except at KW in June and at CH in April and less than $0.1^{\circ}\text{C m}^{-1}$ at the deep stations (Figs.4.5(d-i)). The increased gradient in the coastal regions is due to the combined effect of upwelling which pushes the sub-surface waters towards the surface and net air-sea heat flux and wind mixing which inhibit its upward movement. The low gradients at the deep station is caused by the increased entrainment due to mixing of waters from upper thermocline and mixed layer (Philips,1977). The thermocline gradient more than doubled from pre-monsoon to active monsoon periods both at CH and KW. The thermocline gradient showed an increase from 0.1 to $0.15^{\circ}\text{C m}^{-1}$ in the central Arabian Sea. The thermocline gradient ($\cong 0.1^{\circ}\text{C}$) did not show much variation during both pre-monsoon and monsoon periods at BS and BW.

4.3.2.4 MIXING IN THE THERMOCLINE

Studies on mixing processes indicate that shear and static instabilities are the prime mechanisms governing the gradient in the thermocline (Miles,1961). As Richardson number (Ri) is the ratio of buoyancy to shear term, the thermocline stratification is studied in terms of Ri.

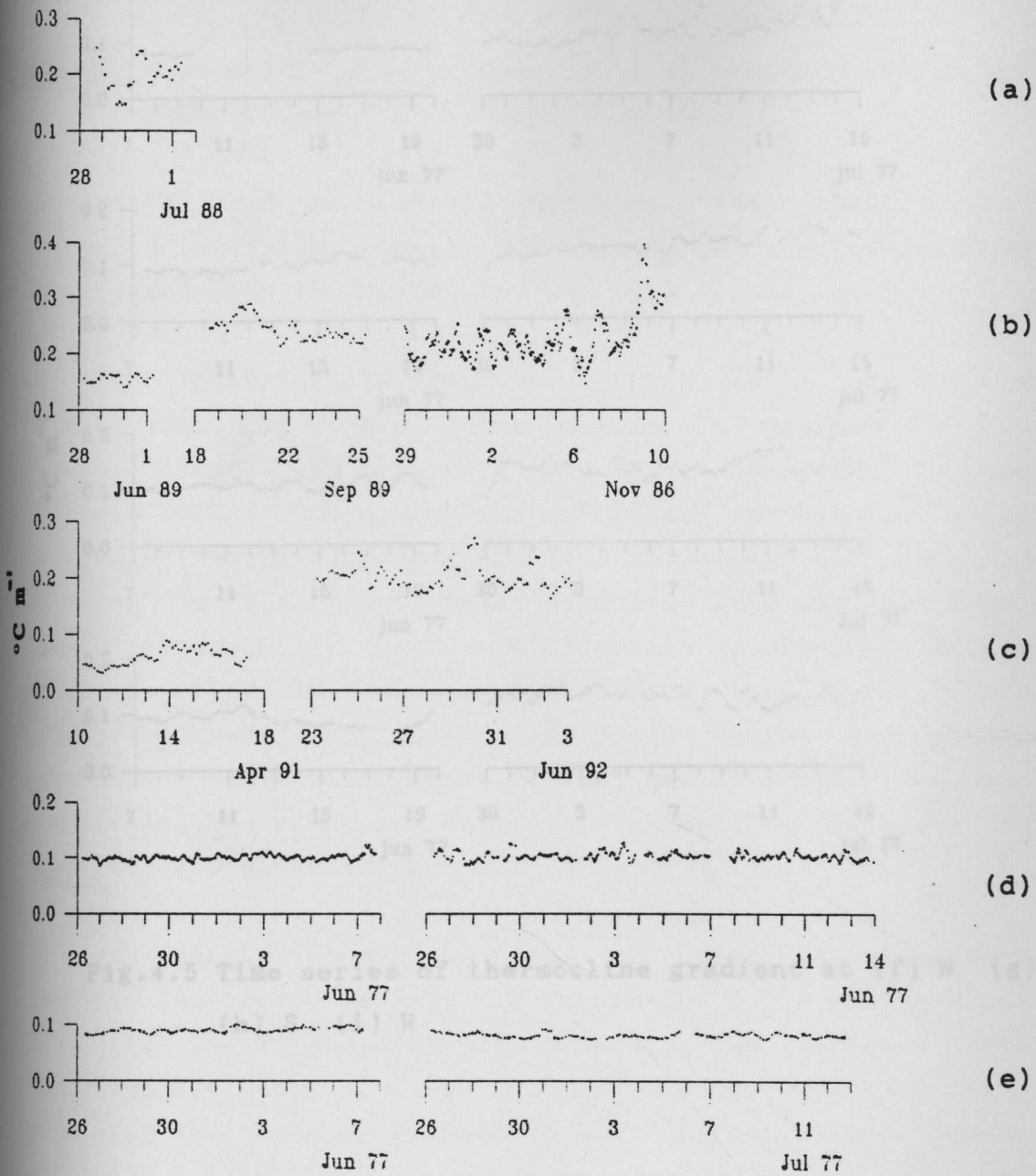


Fig.4.5 Time series of thermocline gradient at (a) BM (b) KW (c) CH (d) BS (e) BW

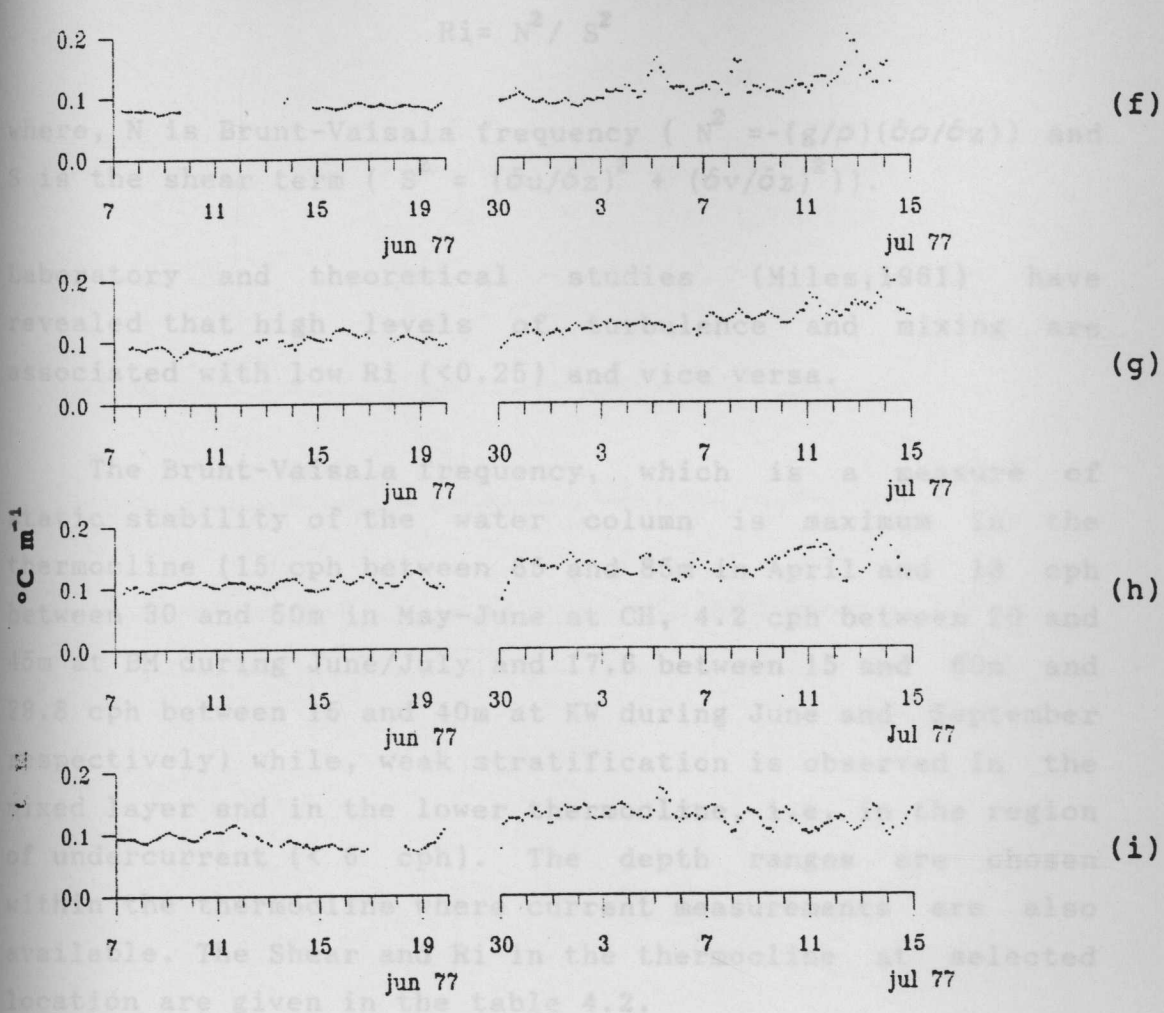


Fig.4.5 Time series of thermocline gradient at (f) N (g) E
(h) S (i) W

$$Ri = N^2 / S^2$$

where, N is Brunt-Vaisala frequency ($N^2 = -(g/\rho)(\delta\rho/\delta z)$) and S is the shear term ($S^2 = (\delta u/\delta z)^2 + (\delta v/\delta z)^2$).

Laboratory and theoretical studies (Miles, 1961) have revealed that high levels of turbulence and mixing are associated with low Ri (< 0.25) and vice versa.

The Brunt-Vaisala frequency, which is a measure of static stability of the water column is maximum in the thermocline (15 cph between 65 and 85m in April and 18 cph between 30 and 50m in May-June at CH, 4.2 cph between 20 and 45m at BM during June/July and 17.6 between 15 and 60m and 28.8 cph between 15 and 40m at KW during June and September respectively) while, weak stratification is observed in the mixed layer and in the lower thermocline, i.e, in the region of undercurrent (< 6 cph). The depth ranges are chosen within the thermocline where current measurements are also available. The Shear and Ri in the thermocline at selected location are given in the table 4.2.

In order to obtain the nature of current at different levels, the current sticks off Cochin for April and May-June are presented in Fig.4.6a. In general, the currents were weak in the top 45m ($10-20 \text{ cm s}^{-1}$). The currents were stronger and opposing between 65 and 85m indicating a shear of 0.005 s^{-1} . However, the currents were stronger ($\cong 50 \text{ cm s}^{-1}$) at all levels about 70m in June except between 23-28 June at 30 and 50m. The drastic decrease of current speed from 30 to 50m between 23 and 28 June leads to large shear (0.025 S^{-1}). However the water column is statically stable during both the periods as indicated by negative $\delta\rho/\delta z$ (-0.03 to -0.09 kg m^{-4}). Further, there was a marked

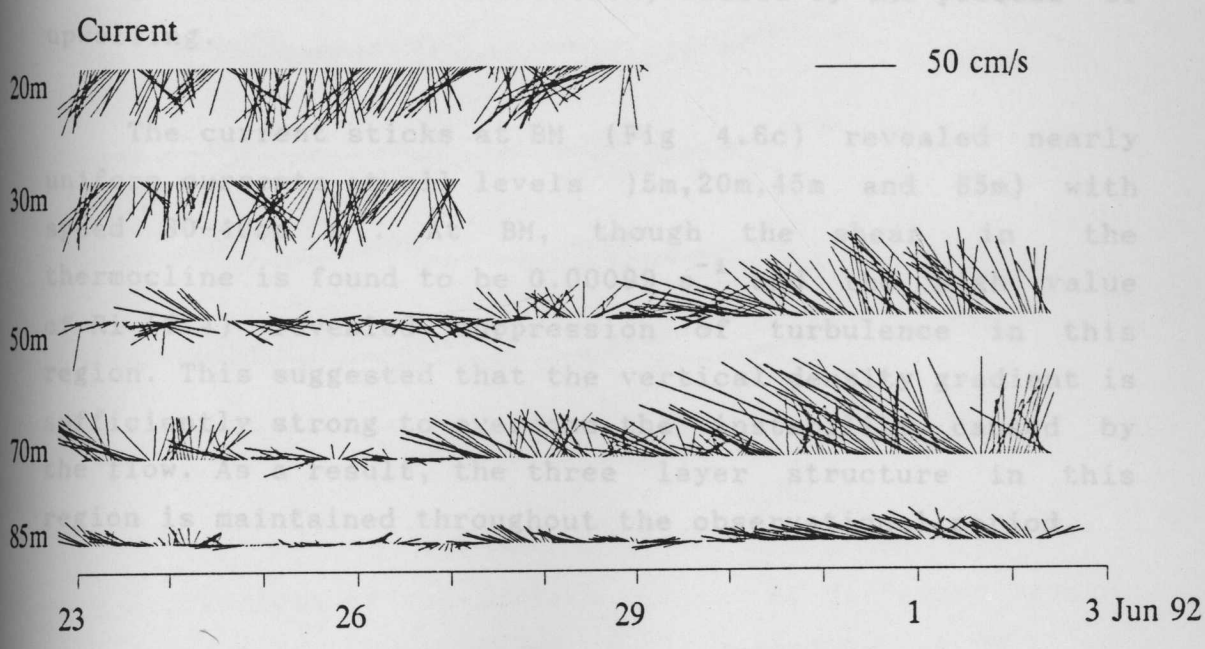
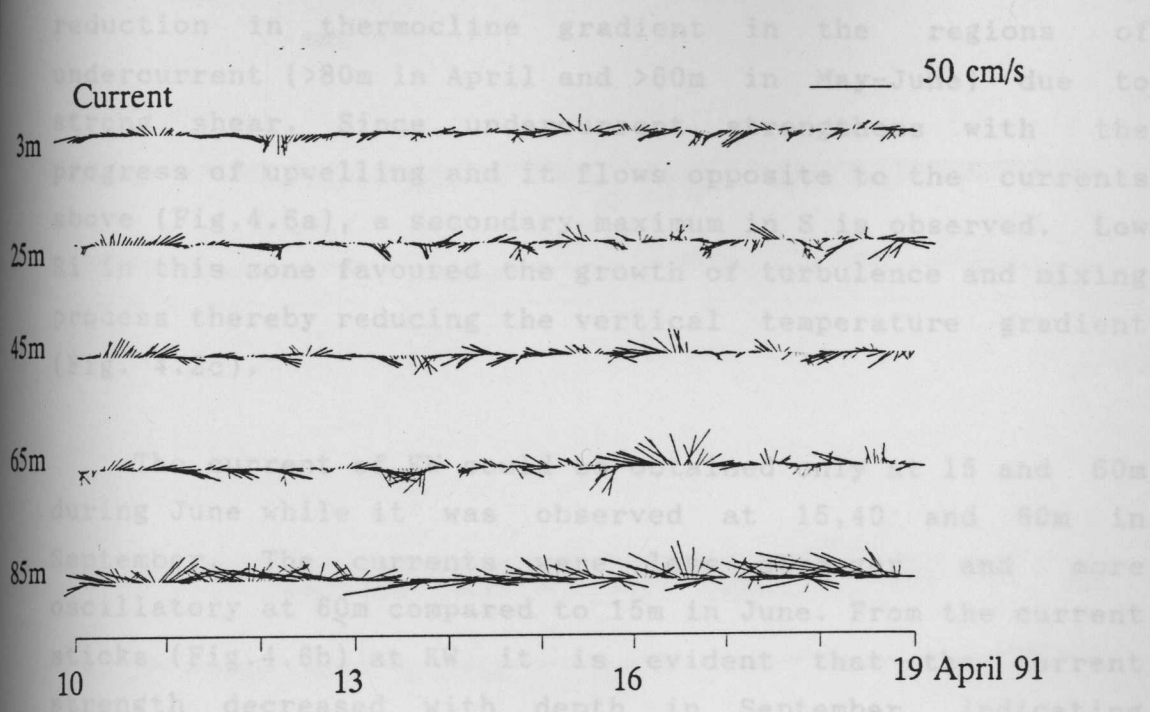


Fig. 4.6 Stick plots of sub-surface current at different levels
 (a) April and May-June at CH

reduction in thermocline gradient in the regions of undercurrent ($>80\text{m}$ in April and $>60\text{m}$ in May-June) due to strong shear. Since undercurrent strengthens with the progress of upwelling and it flows opposite to the currents above (Fig.4.6a), a secondary maximum in S is observed. Low Ri in this zone favoured the growth of turbulence and mixing process thereby reducing the vertical temperature gradient (Fig. 4.2c).

The current of KW could be obtained only at 15 and 60m during June while it was observed at 15,40 and 60m in September. The currents were less stronger and more oscillatory at 60m compared to 15m in June. From the current sticks (Fig.4.6b) at KW it is evident that the current strength decreased with depth in September indicating increased shear. At KW, the strong shear (0.008 s^{-1} in September) is noticed in the thermocline compared to other levels. In June, a low Ri (0.075) revealed increased turbulence, resulting in the weakening of thermal stratification. However, in September Ri (>0.29) indicated suppression of turbulence in the water column, suggesting a strong thermocline stratification, caused by the process of upwelling.

The current sticks at BM (Fig 4.6c) revealed nearly uniform currents at all levels (5m,20m,45m and 65m) with speed $30\text{-}40\text{cm s}^{-1}$. At BM, though the shear in the thermocline is found to be 0.00099 s^{-1} and the high value of Ri (7.4) revealed suppression of turbulence in this region. This suggested that the vertical density gradient is sufficiently strong to overcome the instability caused by the flow. As a result, the three layer structure in this region is maintained throughout the observational period.

4.6 Stick plots of sub-surface current at different levels

(b) July-September at KW (c) June-July at BM

Table 4.2

Average shear (S), Richardson number (Ri) and Brunt-Vaisala frequency (N) at selected locations.

50 cm/s

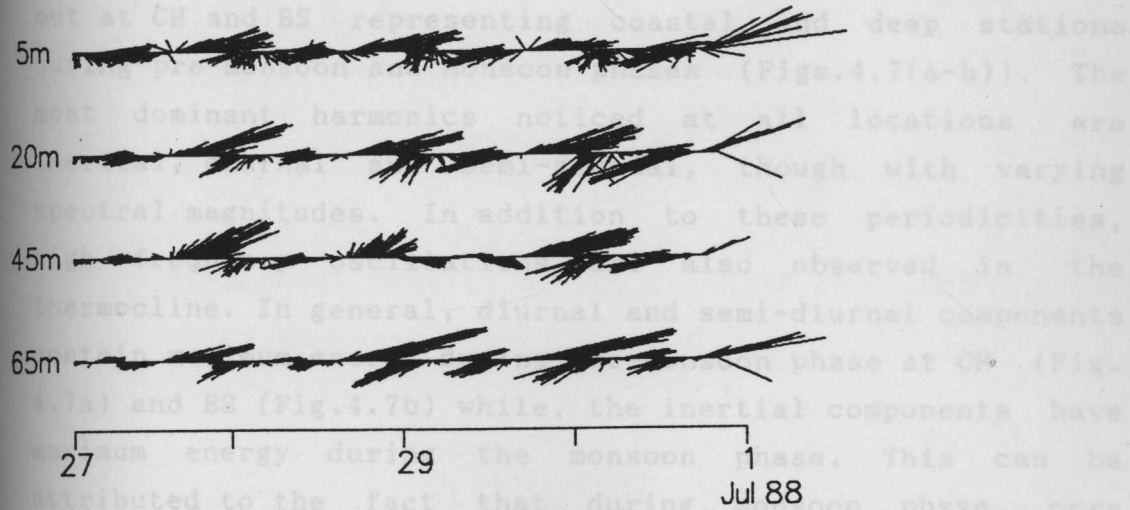
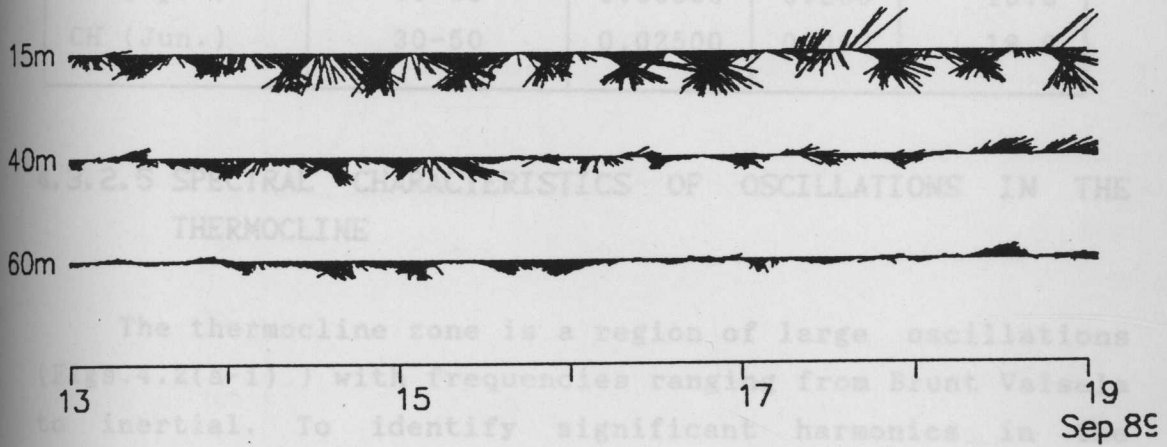
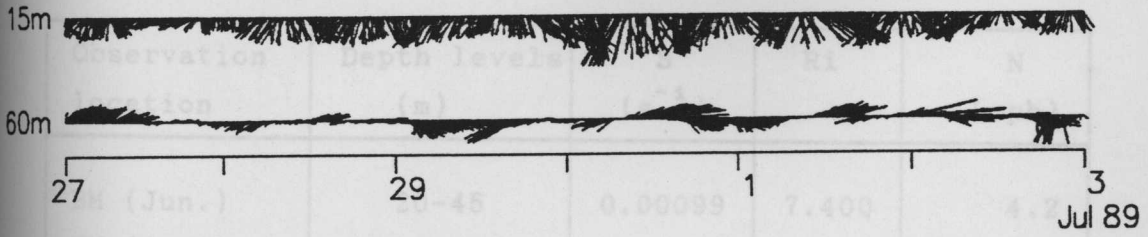


Fig. 4.6 Stick plots of sub-surface current at different levels
 (b) July-September at KW (c) June-July at BM

Table 4.2

Average shear (S), Richardson number (Ri) and Brunt-Vaisala frequency (N) at selected locations.

Observation location	Depth levels (m)	S (s^{-1})	Ri	N (cph)
BM (Jun.)	20-45	0.00099	7.400	4.2
KW (Jun.)	15-60	0.00490	0.075	17.6
KW (Sep.)	15-40	0.00800	0.290	28.8
CH (Apr.)	65-85	0.00500	0.200	15.0
CH (Jun.)	30-50	0.02500	0.050	18.0

4.3.2.5 SPECTRAL CHARACTERISTICS OF OSCILLATIONS IN THE THERMOCLINE

The thermocline zone is a region of large oscillations (Figs.4.2(a-i)) with frequencies ranging from Brunt Vaisala to inertial. To identify significant harmonics in the thermocline, the time series of the depth of 25°C isotherm was subjected to FFT analysis . The analysis were carried out at CH and BS representing coastal and deep stations during pre-monsoon and monsoon phases (Figs.4.7(a-b)). The most dominant harmonics noticed at all locations are inertial, diurnal and semi-diurnal, though with varying spectral magnitudes. In addition to these periodicities, high frequency oscillations are also observed in the thermocline. In general, diurnal and semi-diurnal components contain maximum energy during pre-monsoon phase at CH (Fig. 4.7a) and BS (Fig.4.7b) while, the inertial components have maximum energy during the monsoon phase. This can be attributed to the fact that during monsoon phase, more energy is utilised to disturb strong thermocline

stratification (Fig.4.2b). Moreover, the inertial oscillation (70.9 hrs at CH; 53.3 hrs at BS) noted during the summer monsoon phase, is absent (Fig.4.7a) or weak (Fig.4.7b) during pre-monsoon. This can be due to the fact that, during the monsoon phase, the strong winds blow in pulses, which is favourable for the generation of inertial oscillations. The diurnal and semi-diurnal components energy in the coastal region mainly caused by the internal tides during the pre-monsoon phase.

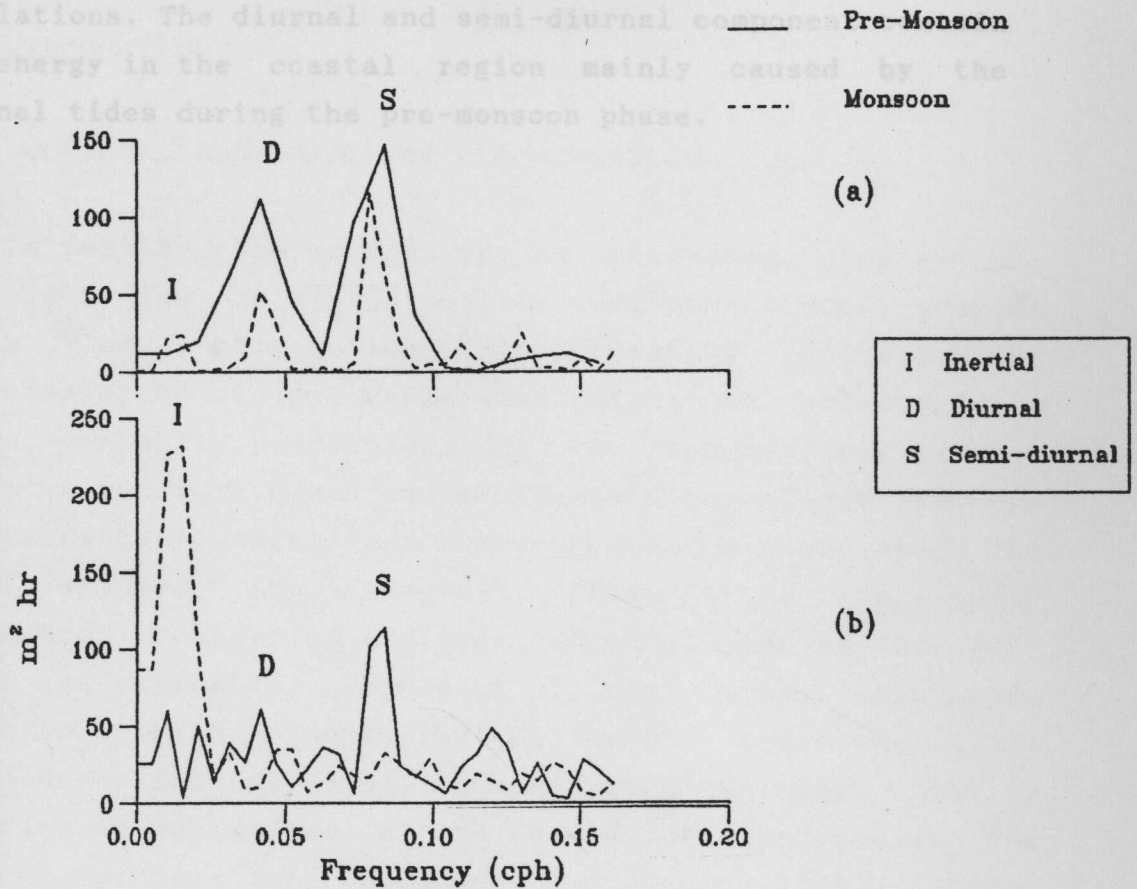


Fig. 4.7 Spectral density of the depth of 25°C isotherm at (a) CH
(b) BS

stratification (Fig.4.2b). Moreover, the inertial oscillation (70.9 hrs at CH;53.3 hrs at BS) noted during the summer monsoon phase, is absent (Fig.4.7a) or weak (Fig.4.7b) during pre-monsoon. This can be due to the fact that, during the monsoon phase, the strong winds blow in pulses, which is favourable for the generation of inertial oscillations. The diurnal and semi-diurnal component contain more energy in the coastal region mainly caused by the internal tides during the pre-monsoon phase.

5.1.1 Oceanic inhomogeneities and acoustics

In reality, the ocean is an extremely complex and variable medium. In such a complex environment more complex models of propagation incorporating statistical characteristics of the variations might be necessary to obtain reliable predictions of the sound field. Ocean currents, internal waves and small-scale turbulence perturb the horizontally stratified character of the sound speed and cause spatial and temporal fluctuations in sound propagation. Boundaries of large currents, such as the Gulf Stream and Kuroshio, represent frontal zones separating watermasses with essentially different characteristics. Within these frontal zones, temperature, salinity, density and sound speed suffer strong variations and hence the acoustic propagation (Levenson and Doblar, 1976). Large eddies in the ocean are mostly observed near intense frontal currents. The parameters of synoptic eddies vary over rather wide range. The diameter of an eddy ranges from 35 to 500km. Analysis of propagation studies through a cyclonic Gulf Stream eddy revealed considerable variations in the propagation conditions (Vastano and Owens, 1973). Considerable fluctuations of the intensity and phase of sound waves arise in the presence of internal waves (Stanford, 1974). We know that such characteristics of the